00017

FINAL REPORT

CONTRACT NO. NAS 7-539

A STUDY OF LIQUID MERCURY ISOLATOR DEVELOPMENT

SEPTEMBER 1967

prepared for

NATIONAL AERONAUTICS AND SPACE ADMINISTRATION
PASADENA, CALIFORNIA

by

J. H. MOLITOR, H. J. KING & S. KAMI

HUGHES
HUGHES AIRCRAFT COMPANY
RESEARCH LABORATORIES
3011 MALIBU CANYON ROAD
MALIBU, CALIFORNIA 90265

A STUDY OF LIQUID MERCURY ISOLATOR DEVELOPMENT

FINAL REPORT

Contract NAS 7-539

by

J. H. Molitor, H. J. King, and S. Kami
Hughes Research Laboratories
A Division of Hughes Aircraft Company
Malibu, California

September 1967

prepared for

NASA – PASADENA OFFICE
PASADENA, CALIFORNIA

TABLE OF CONTENTS

LIST OF ILLUSTRATIONS

SECTION I

INTRODUCTION

This study represents one facet of a much larger program to demonstrate the feasibility of using solar-electric propulsion for a variety of space missions. To date, complete vehicle designs have been evolved,[1] payload advantages for a number of missions have been reported, and the reliability of the various subsystems has been estimated.[2] In most cases, these studies have been based on an electron bombardment thruster using a thermionic cathode and mercury propellant. A very promising alternative electron source which has demonstrated an extremely long useful lifetime is the liquid mercury (LM) cathode.[3] Comparative designs have shown that a system based on the LM cathode is similar to the thermionic cathode thruster in weight, power, and propellant efficiency and in power conditioning and control system requirements. However, there are fundamental differences between these devices in thermal and propellant feed system design. The difference in feed system design results because the LM cathode requires that liquid mercury be supplied to the cathode under relatively high pressure (30 to 150 psi), while the thermionic cathode thruster requires mercury vapor at pressures varying from 10^{-4} to 10 Torr, depending on design. The effect on system design of supplying liquid mercury to the thruster was investigated in this program.

The studies referred to above have demonstrated the advantages of a modularized system (i.e., a total propulsion system comprising a number of completely independent thruster and power conditioning subsystems) for unmanned interplanetary missions. Although it is desirable that the propellant storage reservoirs be modularized as well, propellant in any tank must be accessible to any thruster during the flight.

There are two basic reasons for subsystem modularization. First, modularization allows for the employment of partial redundancy to increase system reliability. In most cases, this option will result in lower system weight for a desired over-all system reliability. The second advantage is the ability to match closely the load (i.e., the thruster array) to the time varying input power of a solar panel without requiring that the power level of individual thrusters vary over extremely large ranges. For example, in a Mars mission the available power from a given solar array varies by more than a factor of two during the mission. If the thrusters are simply turned off at the appropriate time, the load may be closely matched to the available power at all times. In order that this modular concept may be effectively implemented, each thruster subsystem must be electrically independent of the others in the array.

A number of system concepts which provide varying degrees of electrical isolation were investigated in this program. The weight and reliabilities of each were compared with a simple reference system which provides no electrical isolation between subsystems.

The first section of this report contains a complete system analysis which evaluates the weight and reliability of several possible system configurations. This study has been conducted in such a manner that the difference in performance is immediately apparent between an electrically coupled system and those with varying degrees of electrical isolation possible. A number of unique components were required for the design and evaluation of the various systems considered. Although these components were conceptually simple, they did not exist in the form of useful hardware. To alleviate this problem and to provide a basis for weight and reliability estimates of the major components, a hardware development program was implemented. The following components were designed and tested:

1. an isolator — a device which, when inserted in the propellant feed line, permits free passage of liquid mercury but introduces an electrical discontinuity in the line

2. an electromagnetic pump or pressurizer — a device which permits the pressure in individual propellant lines to be adjusted electrically (in this specific case by the use of Lorenz forces).

3. an insulating valve — a device which provides an electrical discontinuity in the propellant line only when flow is stopped.

The design, fabrication, and 100 hour test of the isolator was a goal of the contract. A knowledge of the weight and reliability of a liquid mercury isolator makes generally applicable here the system studies performed earlier for an oxide cathode thruster system (which utilizes an existing mercury vapor isolator). The goal of the hardware program on isolating valves and the electromagnetic pressurizer was to demonstrate feasibility and to provide a basis for weight and reliability estimates discussed earlier.

SECTION II

SYSTEM ANALYSIS

The purpose of the study phase of this program was to determine the effect on system performance (i.e., reliability and weight) of employing some form of electrical isolation between thrusters. Thus, it was necessary to determine the reliability and weight of the various system configurations in which electrical isolation is provided and to compare them with an electrically coupled system.

Certain preliminary steps were essential to the development of the mathematical models required to perform this analysis. First, it was necessary to establish the boundary conditions defining the mission and the basic system to be considered. It was then necessary to identify the many system configurations which are possible when such variables as (1) method of electrical isolation, (2) type of power supply design (i.e., modular or nonmodular), (3) type of electrical hookup (i.e., common power supply or power supply for each thruster), and (4) type of propellant storage system (i.e., single or multiple reservoir) are combined. Finally, before the development of the mathematical models could begin, it was necessary to reach certain decisions in order to reduce the number of systems to some manageable number for analysis.

In concurrence with the JPL program manager, it was agreed that the following ground rules would be used for this study:

1. The example mission would be a Jupiter flyby in the year 1973.

2. The propulsion system would comprise eight 2.6 kW mercury bombardment ion thrusters employing a liquid mercury pool cathode. Based on reliability considerations, six ion thrusters would be operating initially and two would be standbys.

3. Only six power conditioning and control systems would be provided; because power conditioner reliability can be increased internally, no standby systems would be required. However, it was assumed that these systems would be designed so that each could be switched to any thruster in the array, if required.

4. The propellant reservoir would be sized to hold 865 lb of mercury.

A. SYSTEM CONFIGURATIONS

In order to determine the reliability and weight variations associated with an electrically decoupled thruster system, it was first necessary to determine the system design alternatives which might exist. A study of the problem of providing electrical isolation between thrusters which use liquid mercury propellant systems resulted in the definition of three basic electrical isolation techniques:

1. A separate propellant storage and propellant system could be provided for each thruster

2. Special insulating valves could be developed for use between each thruster and a common propellant storage system. Since such a valve can provide electrical insulation only when closed, it must be used only to isolate thrusters which are turned off or when a separate small auxiliary reservoir must be provided for each thruster. The auxiliary reservoir would be separated from the main storage reservoir by the insulating valve. The valve would then be kept closed except when propellant was being transferred to the auxiliary reservoir

3. An isolator would be developed to provide an electrical discontinuity in the flowing stream of liquid mercury propellant (e.g., the bubble isolator described in Section III).

When the isolation methods described above (plus a coupled system for reference) were combined with the variables of common or separate power supplies, modular or nonmodular power supply design, and single or multiple storage reservoirs, the number of system configurations reached 32. Each of these configurations was then evaluated in terms of its ability to satisfy such requirements as isolation while a thruster is operating, individual pressure regulation without an electromagnetic pump, transfer of propellant between reservoirs, storage system at spacecraft ground potential, ease of faulty thruster identification, and available propellant for standby thrusters without extra reservoirs. Based on this evaluation, and with concurrence from JPL, it was agreed to eliminate from consideration those configurations which included either a common power supply or nonmodular separate power supplies. (However, the coupled common power supply reference system was not eliminated.) As a result of this preliminary evaluation, the original 32 system configurations were reduced to the eight shown in Fig. 1.

Of the eight system configurations selected for analysis, three are insulating valve systems utilizing a separate storage reservoir for each thruster (systems A-1, A-2, A-3 in Fig. 1); two are insulating valve systems in which the number of storage reservoirs is independent of the number of thrusters (B-1, B-2); two are isolator systems (C-1, C-2); and one is the nondecoupled reference system (D-1). Three systems are necessary in the insulating valve category because of the possible variation in system characteristics when conventional valves are combined with insulating valves. For example, system A-1 does not provide isolation while the thruster is operating (and for this reason it requires a variable impedance in series with thruster load), but it provides isolation of a failed thruster without also blocking off the associated reservoir.

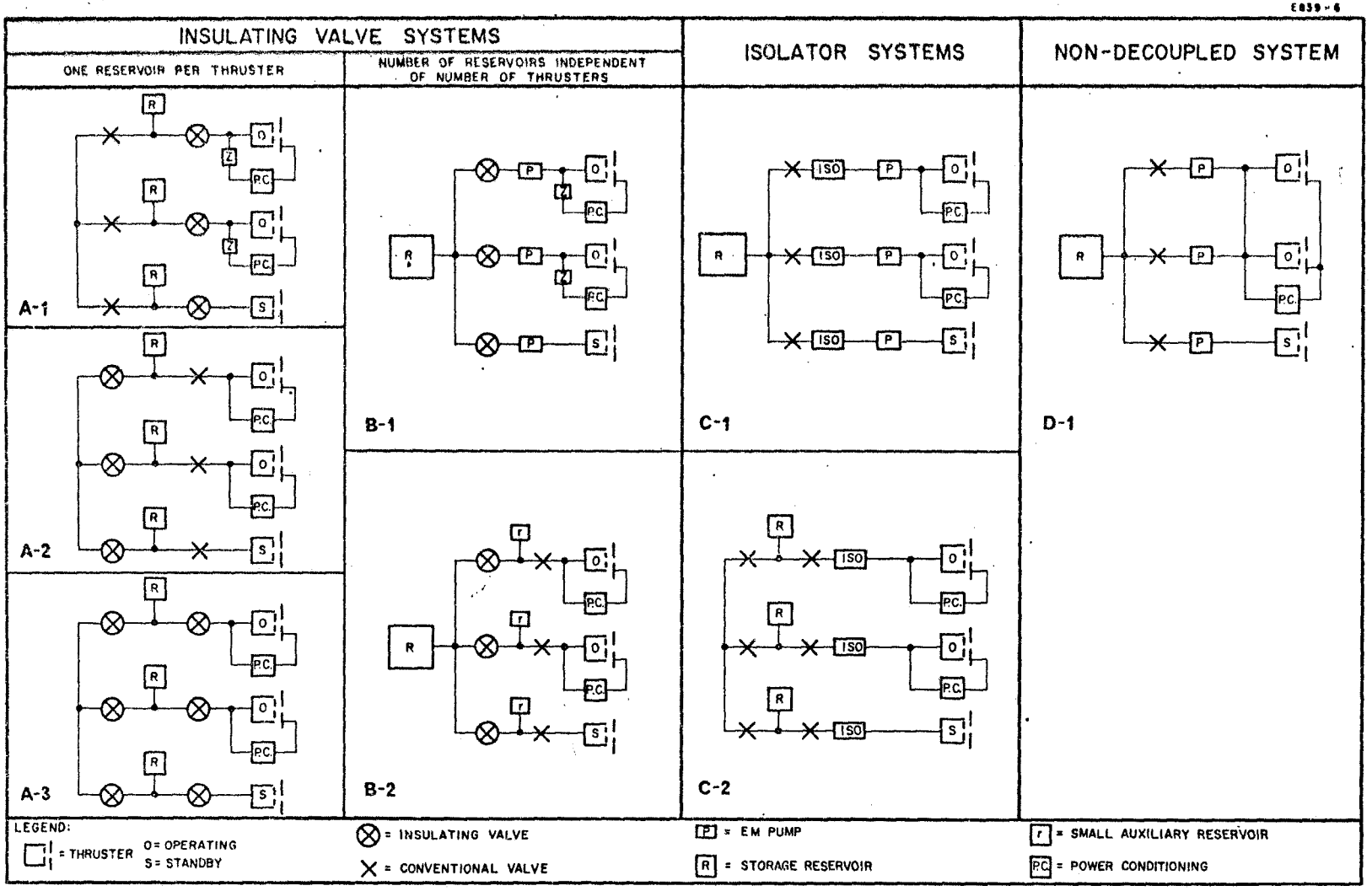

Fig. 1. Reliability and weight model schematic diagrams.

These two conditions are reversed for system A-2 because the positions of the isolating and conventional valves are interchanged. The third system in this category (A-3) uses all insulating valves. Therefore, while it provides both of the desirable features of the previous two, it also represents a different system from a reliability and weight standpoint (since conventional and insulating valves are found to have different failure rates and weights).

The two insulating valve systems in which the number of reservoirs is independent of the number of thrusters differ in the method of propellant pressure control for the individual thrusters. System B-1 utilizes an EM pump for this function. System B-2 accomplishes pressure regulation by operating each thruster from a separate small auxiliary reservoir which is isolated from the storage reservoir by an insulating valve which is closed except when the auxiliary reservoir is being filled.

The two isolator systems have the following differences: in C-1, the number of storage reservoirs is independent of the number of thrusters; system C-2 has one reservoir for each thruster. As was true for the previous category, some means of pressure control is required when the number of storage reservoirs is independent of the number of thrusters. In system C-1, electromagnetic pumps are used.

Inspection of Fig. 1 shows that the eight system configurations can be classified as follows:

1. Systems which require a reservoir for each thruster and provide a power conditioner for each thruster

2. Systems for which the number of reservoirs employed is not determined by the isolation scheme, but which still provide a power conditioner for each thruster

3. The reference system which employs an undefined number of reservoirs and a common power supply.

By classifying ion thruster systems in this way, it is possible to evaluate the reliability and weight of each system configuration through the aid of three reliability and three weight models. Variations of system designs which fall within one of the classifications (as described by the proper mathematical model) can then be handled simply by using appropriate component failure rate and weight values.

The three reliability and three weight models can be generated by considering the block diagrams in Fig. 2.

B. ANALYTICAL MODELS

1. Model No. 1

a. Reliability

Figure 2(a) shows that the Class 1 system configuration can be divided into three reliability elements in series. The over-all system reliability is the product of the reliabilities of these elements. In terms of ion propulsion system components or subsystems, these elements consist of (1) the thruster array (six operating initially and two in standby), including all components which are required for each thruster, such as propellant flow valves and reservoirs (and, in one case, isolators); (2) six power conditioning subsystems; and (3) a propellant manifold.

The reliability R of the first element can be determined by applying the reliability theory for modularized solar-powered ion thruster systems developed in Ref. 1. For completeness, this theory will be reviewed briefly.

E839-8RI

MODEL NO. 1

(a)

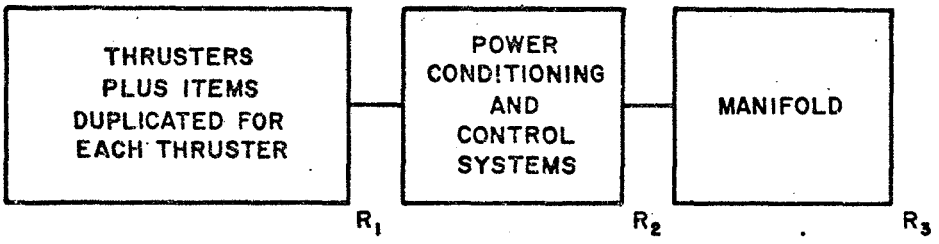

$$R_s = R_1 \cdot R_2 \cdot R_3$$

MODEL NO. 2

(b)

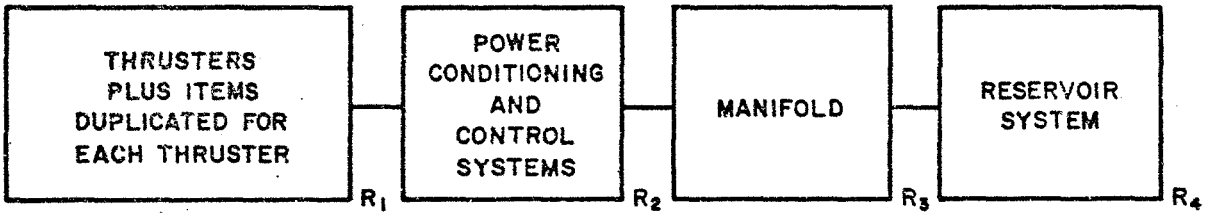

$$R_s = R_1 \cdot R_2 \cdot R_3 \cdot R_4$$

MODEL NO. 3

(c)

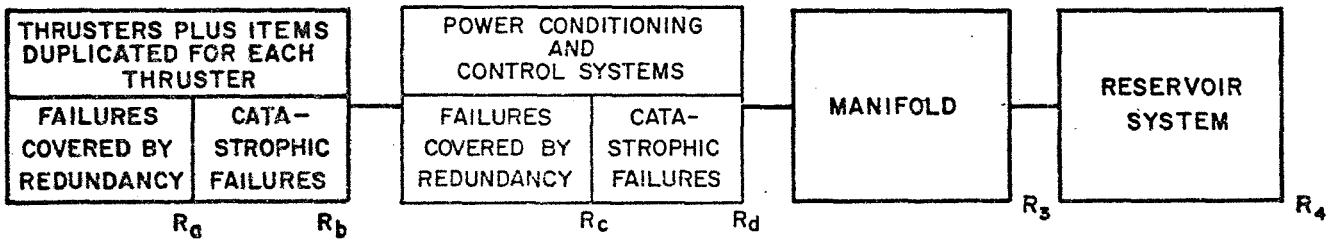

$$R_s = (R_a \cdot R_b) \cdot (R_c \cdot R_d) \cdot R_3 \cdot R_4$$

Fig. 2. Reliability model block diagrams.

The reliability theory for modularized ion thruster systems is based on an extension of the classical concepts currently used in reliability engineering. As discussed in Ref. 1, the only applicable technique for increasing the reliability of a thruster system is standby redundancy.

It was also shown in Ref. 1 that because of variations in the available power and output voltage of the solar panel, thruster and power conditioning modules will be switched during the mission. In each case, the modules and their respective subsystems are designed so that disconnected modules can be reinstated. From the point of view of reliability, the shutdown modules can then be considered as standbys.

Since solar-electric propelled spacecraft in their heliocentric trajectories generally can travel toward and then away from the sun, the reliability analysis of a standby redundant modularized system must include missions in which modules are turned both on and off at different times. As will be shown, the times when modules are turned on and those when they are turned off can be analyzed separately and then fitted together at the proper points in the proper sequence.

(1) Adding Modules — Assume that there are m_o operating and n_o standby modules at $t = 0$ and that an additional module is turned on at times t_μ, $\mu = 1, 2, \ldots, \nu$. The reliability $R(t_\mu)$ of the system in $(0, t_\mu)$ can be calculated as follows. By definition, let

$P_n(t_\mu) \equiv$ probability that exactly n failures occur in $(t_{\mu-1}, t_\mu)$

$r_n(t_\mu) \equiv$ probability that exactly n failures occur in $(0, t_\mu)$.

From these definitions, it is clear that $r_n(t_1) = P_n(t_1)$. For other values of μ, $r_n(t_\mu)$ may be calculated recursively using the relation

$$r_n(t_\mu) = \sum_{\alpha=0}^{n} r_\alpha(t_{\mu-1})\, P_{n-\alpha}(t_\mu) \quad . \tag{1}$$

The system reliability $R(t_\mu)$ may then be found from

$$R(t_\mu) = \sum_{n=0}^{m_o} r_n(t_\mu) \quad . \tag{2}$$

(2) Turning Off Modules — Assume that there were m_o operating and n_o standby modules at $t = 0$ and that ν modules have been turned on, the last at time t_ν. Now it is desired that modules be turned off, one at each of the times $t_{\nu+1}, t_{\nu+2}, \ldots, t_{\nu+k-1}$, and that the reliability $R(t_k)$ at the end of this mission be known. Using the method described previously, the probabilities $r_n(t_{\nu+\mu})$ can be determined for $n = 0, 1, \ldots, n_o + \mu - 1$. Remembering that one operating module becomes a standby at time $t_{\nu+\mu}$, it is seen that the probabilities $r_n(t_{\nu+\mu})$ are given by

$$r_n(t_{\nu+\mu}) = \sum_{a=0}^{n} P_a(t_{\nu+\mu})\, r_{n-a}(t_{\nu+\mu-1}); \quad n = 0, 1, \ldots, n_o + \mu - 1 \quad , \tag{3}$$

provided that

$$r_{n_o+\mu}(t_{\nu+\mu}) = 0; \quad \mu = 1, 2, \ldots k \quad . \tag{4}$$

With a similar recursion for the other r_n's, the mission reliability may then be calculated from

$$R(t_k) = \sum_{n=0}^{n_o+k-1} r_n(t_k) \quad . \tag{5}$$

The statistics of the exact number of failures $P_n(t_\mu)$ are taken to be the usual Poisson law

$$P_n(t_\mu) = \frac{e^{-\lambda_\mu \Delta t_\mu} (\lambda_\mu \Delta t_\mu)^n}{n} \tag{6}$$

where

$$\Delta t_\mu = t_\mu - t_{\mu-1} \ , \tag{7}$$

and the failure rate λ_μ is given by

$$\lambda_\mu = (\lambda_p + m_o \lambda_c) \frac{m_o + \mu - 1}{m_o} \qquad \mu = 1, \ldots, \nu \tag{8}$$

$$\lambda_\mu = (\lambda_p + m_o \lambda_c) \frac{m_o + 2\nu - \mu - 1}{m_o} \qquad \mu = \nu + 1, \ldots, \nu + k \tag{9}$$

where

$\lambda_p \equiv$ failure rate of those items dependent on engine size

$\lambda_c \equiv$ failure rate of those items independent of engine size.

(3) Switching Times — It was shown in Ref. 1 that the engine switching times t_μ are determined from the solar panel maximum current curve $I_m(t)$. If I_o is the available current at $t = 0$, the switching times occur when the curve $I_m(t)$ changes from I_o by increments of I_o/m_o. This procedure is illustrated in Fig. 3. The times t_1 and t_2 occur when the current increases to $I_o + I_o/m_o$ and $I_o + 2I_o/m_o$, respectively. The last turn-on time t_ν is determined from the condition that the maximum current $I(t_{max})$ is less than $I_o + (\nu + 1) I_o/m_o$. After $t = t_{max}$, modules are switched off each time the current falls an amount I_o/m_o.

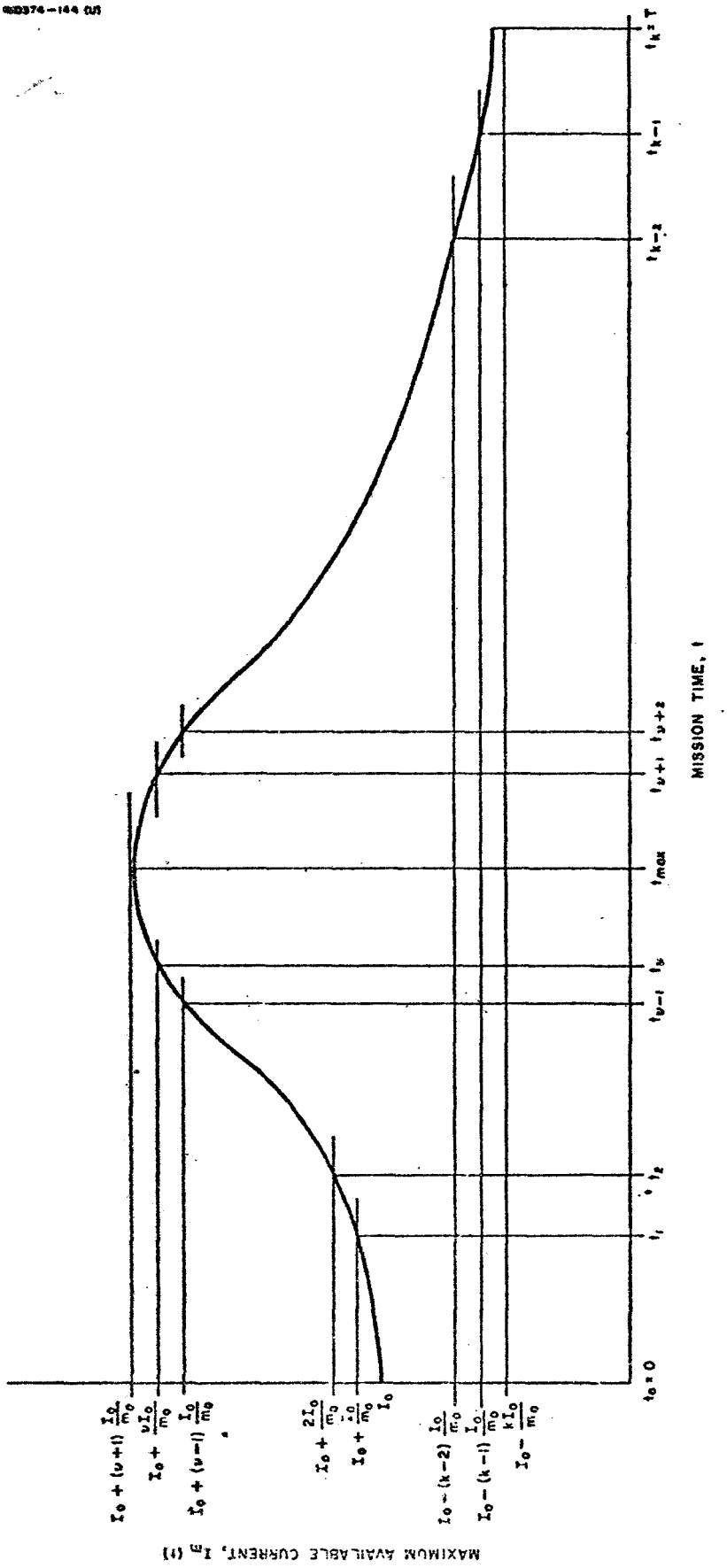

Fig. 3. Representative curve of maximum available current $I_m(t)$ versus time.

The above formulization, which was developed under JPL Contract No. 951144, was computerized and used to determine R_1. The required inputs consisted of the 900 day 1973 Jupiter flyby trajectory data and maximum available power from a solar panel as a function of distance from the sun. The engine switching times listed in Fig. 4 were determined from these data.[1]

The total engine array reliability R_1 for the Jupiter mission, assuming six initially operating thrusters and two standbys, is shown in Fig. 4 as a function of the reliability of a single engine. In this analysis the single engine reliability represents the reliability of the thruster, plus all items duplicated for each thruster. Thus, the value to be assumed for single engine reliability will depend on the system configuration under consideration.

Under the assumption that each of the power conditioning and control panels can be switched to any engine, the reliability R_2 of the second element of Model 1 can also be determined using the above formulation. Figure 5 shows the total power conditioning and control system reliability for a propulsion system which employs six initially operating power conditioners with none in standby.*

The reliability R_3 of the third element is given simply by

$$R_3 = e^{-\lambda_{man} t} \tag{10}$$

where λ_{man} is the failure rate of the propellant manifold.

b. Weight

The weight W_s of the Class 1 system is given by

$$W_s = 8\, W_1 + 6\, W_2 + W_3 \tag{11}$$

where W_1 is the sum of the weights of a single thruster and the components and subsystems which must be duplicated for each thruster, W_2 is the weight of a power conditioning and control unit, and W_3 is the weight of the manifold.

*The general effect of having initial standbys can be seen by comparing Figs. 4 and 5.

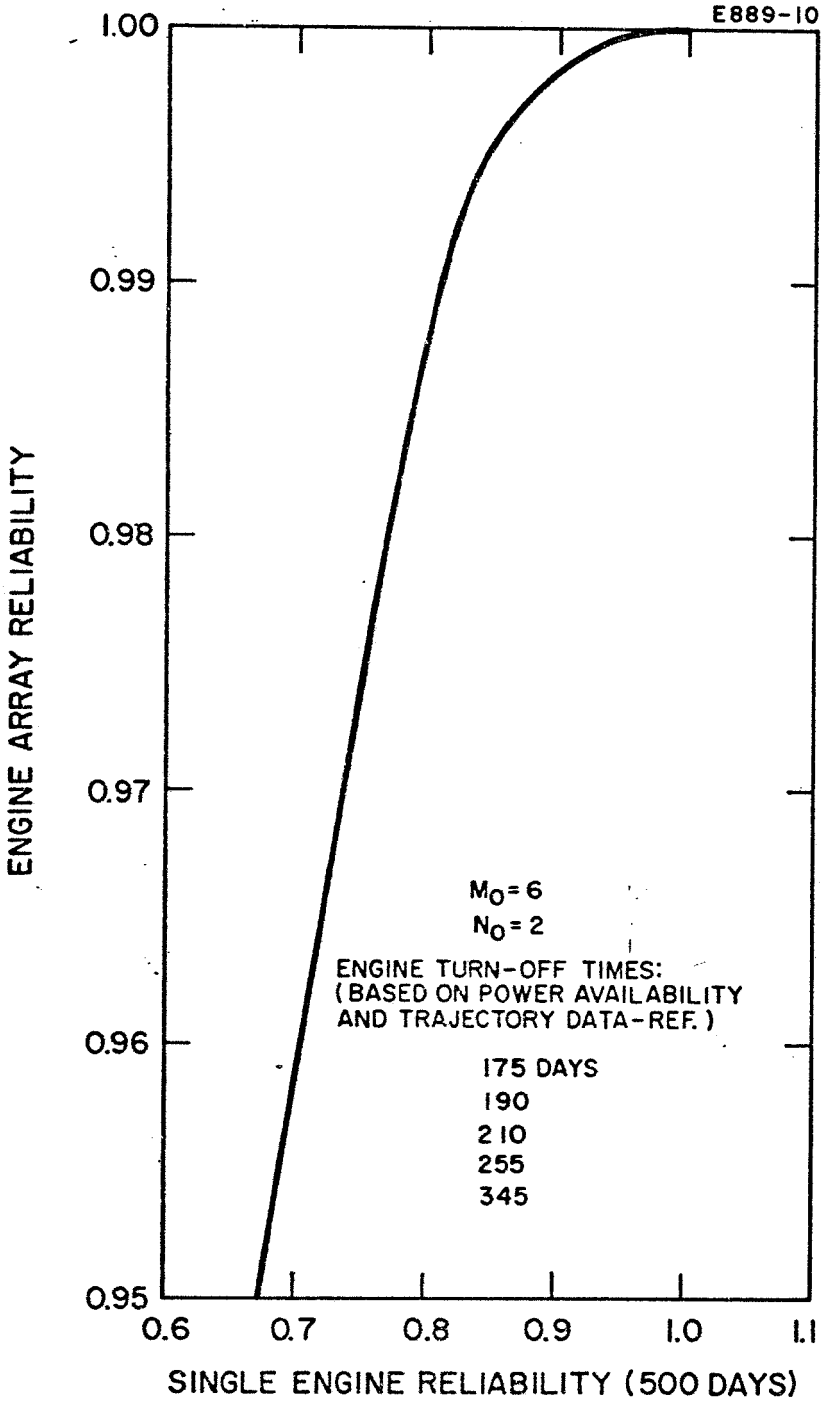

Fig. 4. Engine array reliability for 900 day Jupiter flyby mission (500 day thrusting time).

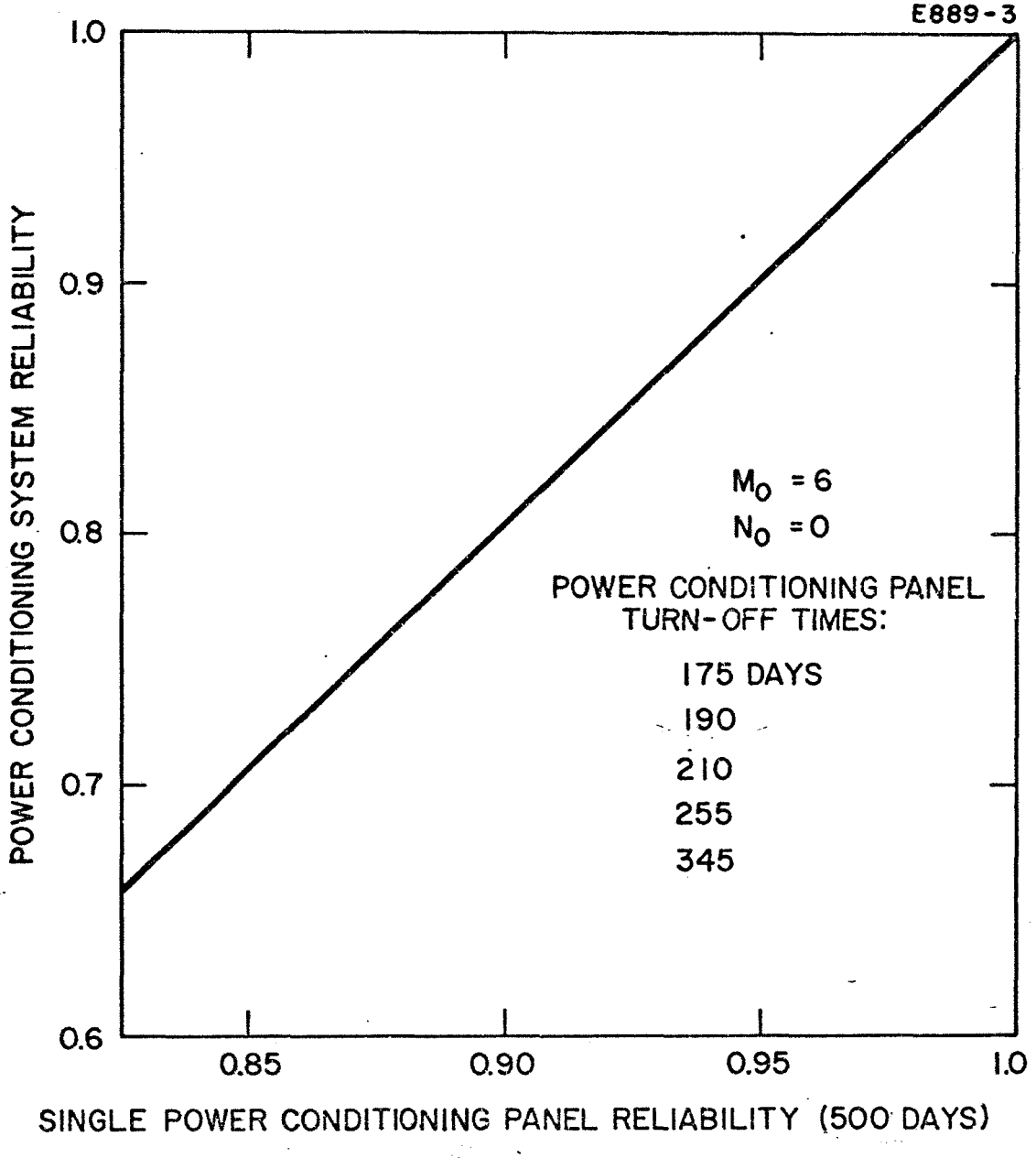

Fig. 5. Power conditioning system reliability for 900 day Jupiter mission (500 day thrusting time).

2. Model No. 2

a. Reliability

Figure 2(b) shows that the Class 2 system configuration can be divided into four elements, with the system reliability given by the product of the reliabilities of these elements. In terms of propulsion system components and subsystems, these elements now consist of (1) the thruster array and all items which must be duplicated for each thruster, such as valves and electromagnetic pumps, valves and small reservoirs, or valves and isolators; (2) the power conditioning units; (3) the manifold; and (4) the reservoir system.

Except for differences in the effective failure rates (because different components might possibly be involved), the reliabilities of elements of (1) through (3) will be given by the reliability models for R_1, R_2, and R_3 presented above. However, the reliability of the reservoir system R_4 must now be determined independently, since it is no longer affected by the number of thrusters employed. In the Class 2 system configuration, the reservoir system can consist of single or multiple propellant tanks. If necessary, it also can provide redundancy in the form of standby tanks (and/or propellant). The "optimum" degree of modularization and redundancy from a weight-reliability standpoint can be determined in the following manner. The reliability of a system in which p units are operating and q are in standby has been shown[2] to be given by

$$R_{p,q} = e^{-p\lambda_p t} \sum_{r=0}^{q} \frac{(p\lambda_p t)^r}{r!} \qquad (12)$$

where λ_p is the failure rate of a reservoir module and is a function of module size.

The total weight of the reservoir system is given by

$$W_{p,q} = (p + q)W_p \qquad (13)$$

where W_p is the weight of a reservoir module and is also a function of module size. Thus, once the functional relationships $\lambda_p = f_1$ (reservoir capacity) and $W_p = f_2$ (reservoir capacity) are determined, a weight-reliability optimization of the reservoir system can be performed.

For the study phase of this program, the reservoir design to be considered will be a gas pressurized, bladder type, spherical tank made of titanium. It will be assumed that the minimum wall thickness is 0.01 in., as dictated by fabrication limitations, and that the tank is pressurized to 30 psi, as required by the liquid mercury cathode. The weight of such a reservoir as a function of liquid mercury storage capacity is shown in Fig. 6. A breakdown of the reservoir weights is provided in Appendix I. From these data, the relationship between the weight of an individual reservoir and the number of tanks employed to contain the 865 lb of mercury required by the mission can be determined as shown in Fig. 7. An estimate of the failure rates of these reservoirs is shown in Fig. 8 as a function of liquid mercury storage capacity. These failure rates were obtained by collecting the failure rates of the various components (or similar components) used to fabricate a complete reservoir subsystem. This breakdown is given in Appendix I. From these data the failure rate of an individual reservoir as a function of the number of tanks employed to store the 865 lb of mercury can be obtained as shown in Fig. 9.

The procedure for determining the optimum reservoir module size, based on a weight-reliability criterion, may be summarized in the following manner. First, the relationships $\lambda_p = f_1(p)$ and $\omega_p = f_2(p)$ (as provided by the data in Figs. 9 and 7) are substituted into (12) and (13), respectively. A desired reservoir system reliability $\overline{R}$ and a range for p are then chosen. For each value of p in its range, the smallest value of q is determined such that

$$R_{p,q} \geq \overline{R} \quad . \tag{14}$$

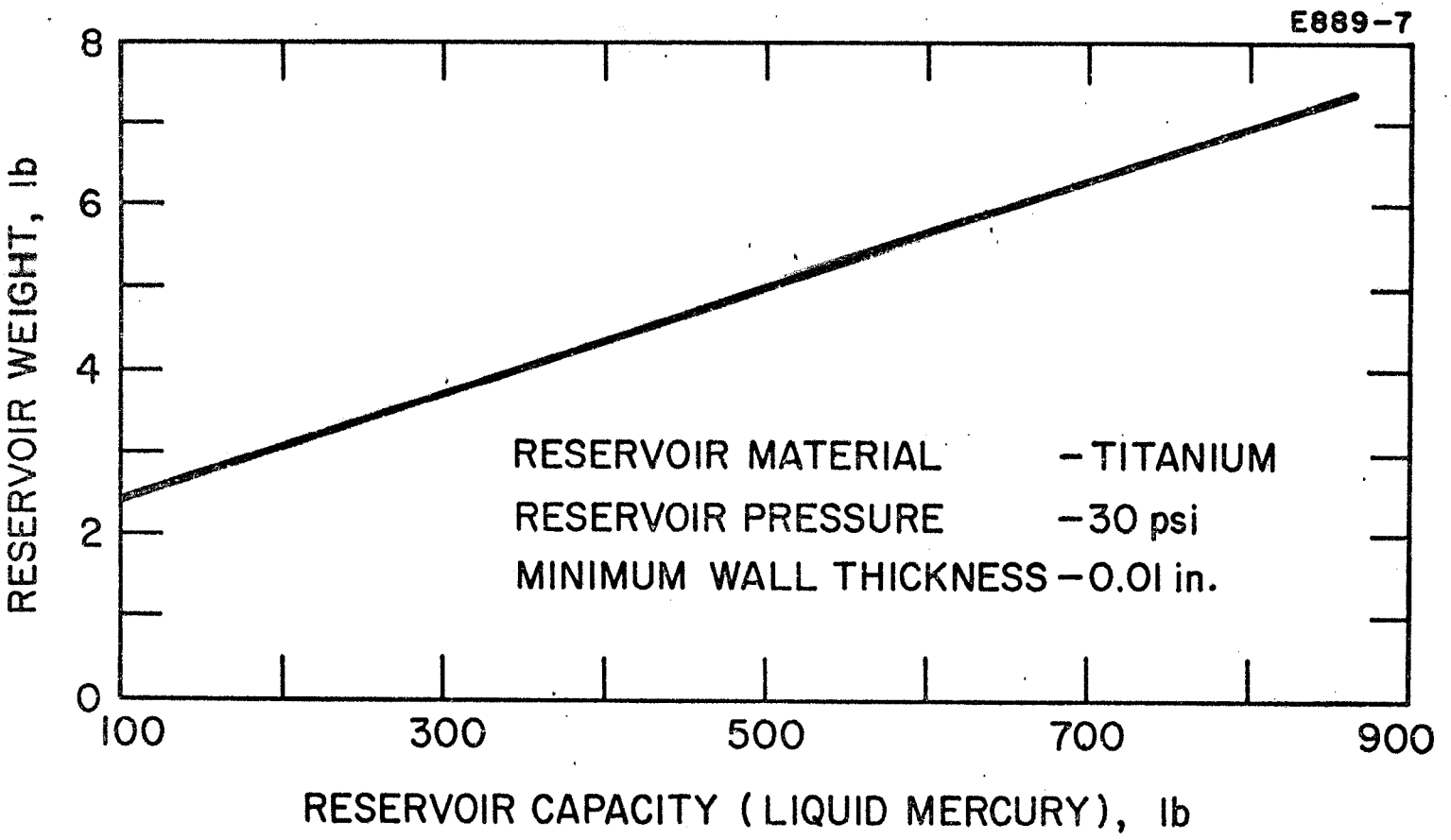

Fig. 6. Reservoir weight for gas pressurized spherical tanks.

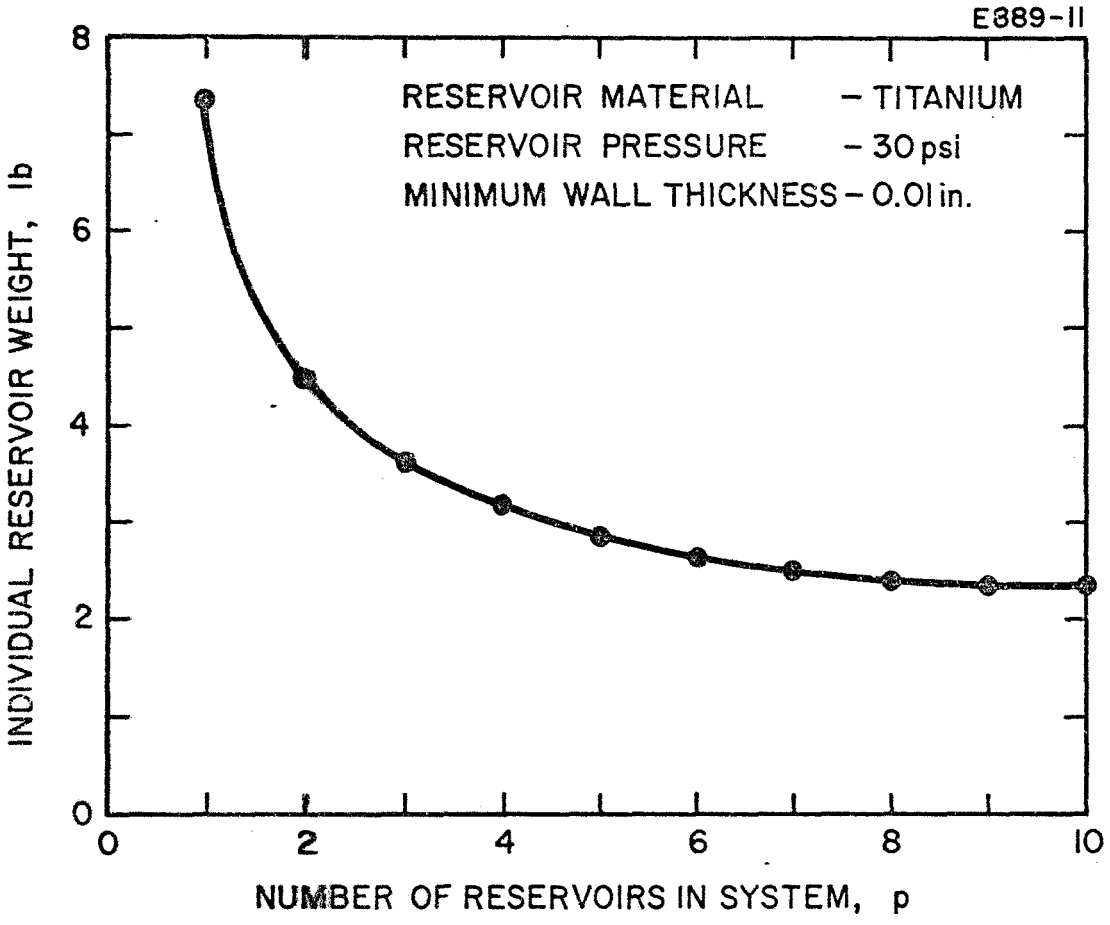

Fig. 7. Single reservoir weight in modularized tankage system (total mercury weight = 865 lb).

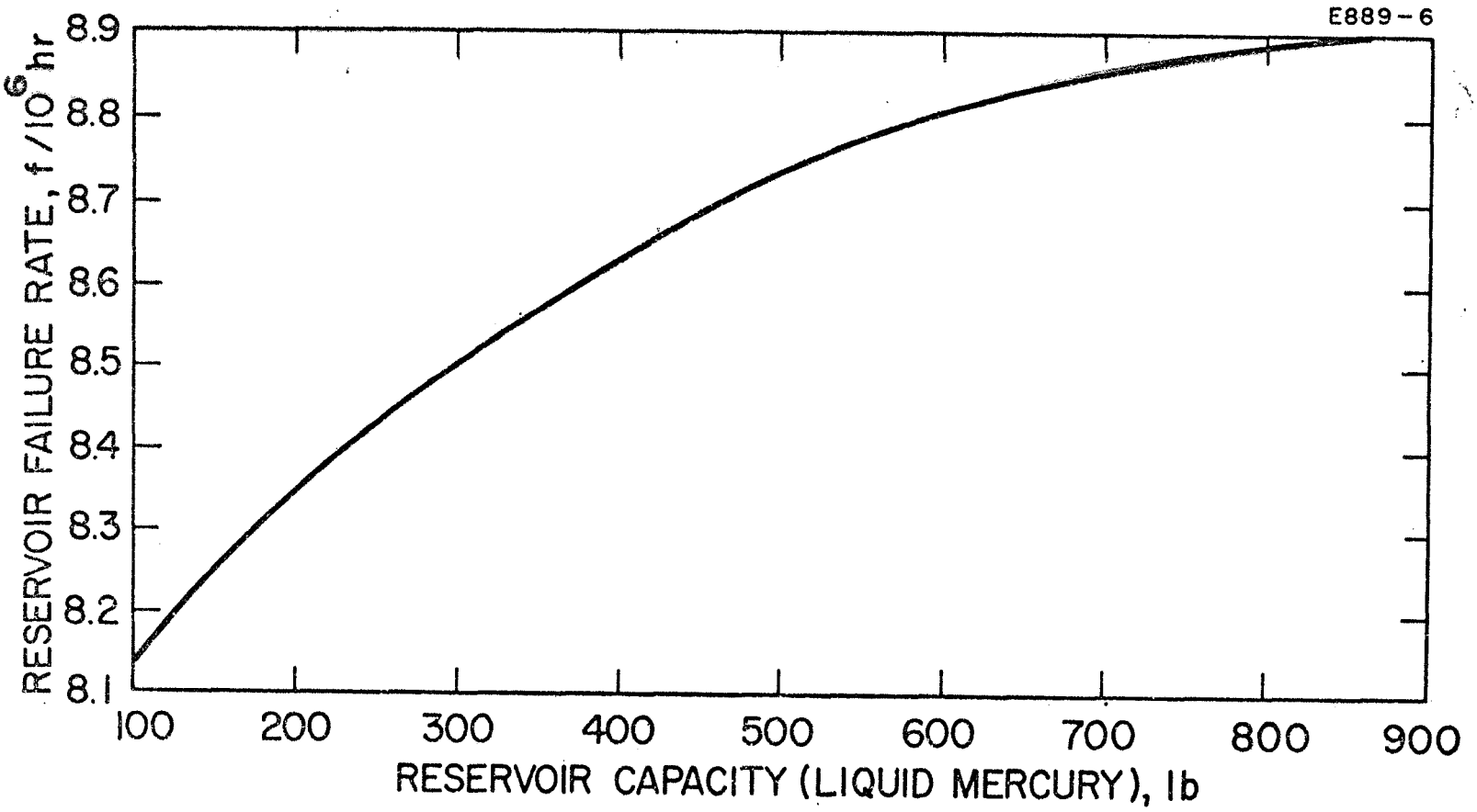

Fig. 8. Reservoir failure rates for gas pressurized spherical tanks.

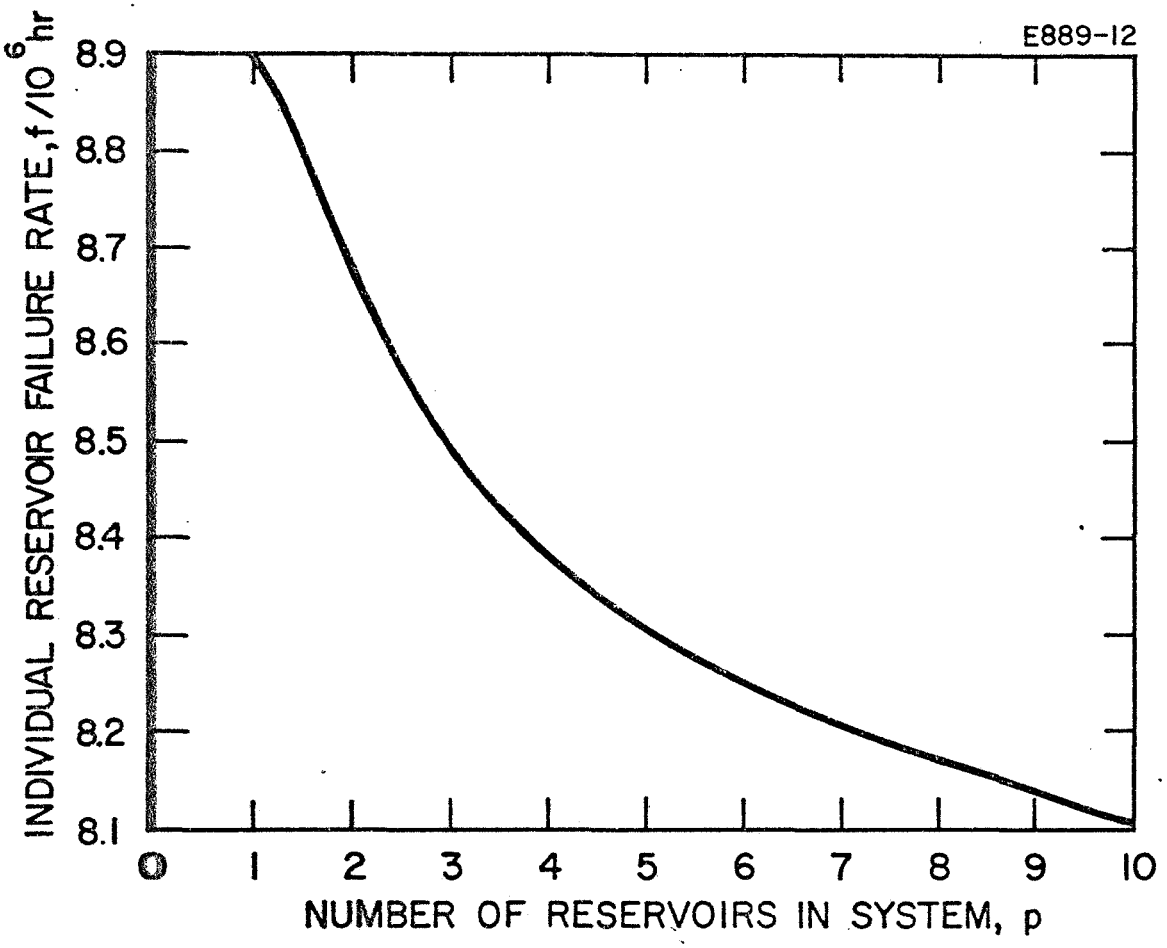

Fig. 9. Single reservoir failure rate in modularized tankage system (total mercury weight = 865 lb).

From the set of operating and standby module pairs (p, q) generated, the optimum is that set at which the total system weight is a minimum.

This weight-reliability otpimization was carried out by computer for reservoir system reliability $\overline{R}$ values from 0.85 to 0.97, using a range of p from 1 to 10. Although the optimum number of reservoirs may be greater than 10 in some situations, from a practical standpoint this was thought to be an appropriate limit. The study was conducted for two possible system designs. In one, the redundant tankage does not contain propellant; in the event of an operating reservoir failure, it is assumed that the remaining propellant can be successfully transferred to the standby tanks. For certain types of failure (i.e., loss of pressurizer, rupture of bladder, etc.) transfer of propellant would not be possible; therefore, this first case may be considered academic. However, the results are presented for the sake of comparison. Since the amount of propellant in this design does not depend on the degree of system modularization or redundancy, the optimum combination of operating and standby tanks (p, q) can be found by considering tankage weight only. The total weight of a modularized reservoir system with standbys is shown in Fig. 10 for $\overline{R}$ values of 0.85, 0.90, and 0.95. Also given is the number of standby tanks required to obtain the desired over-all system reliability for each value of p. For a $\overline{R}$ of 0.85, the minimum weight system occurs when a single operating tank with no standbys is employed. For desired system reliabilities of 0.90 and 0.95, the optimum number of operating reservoirs is two, with one standby unit. The penalty for increasing the tankage system reliability to a value greater than 0.95 (actually to 0.9815 by means of modularization and redundancy from its original value of 0.8988) is only 6 lb.

The second possible (and more probable) configuration assumes that in a failure in an operating reservoir, the propellant in that tank is lost; thus, all standby tanks must contain a full propellant load. Therefore, the optimization procedure must now consider the effect of

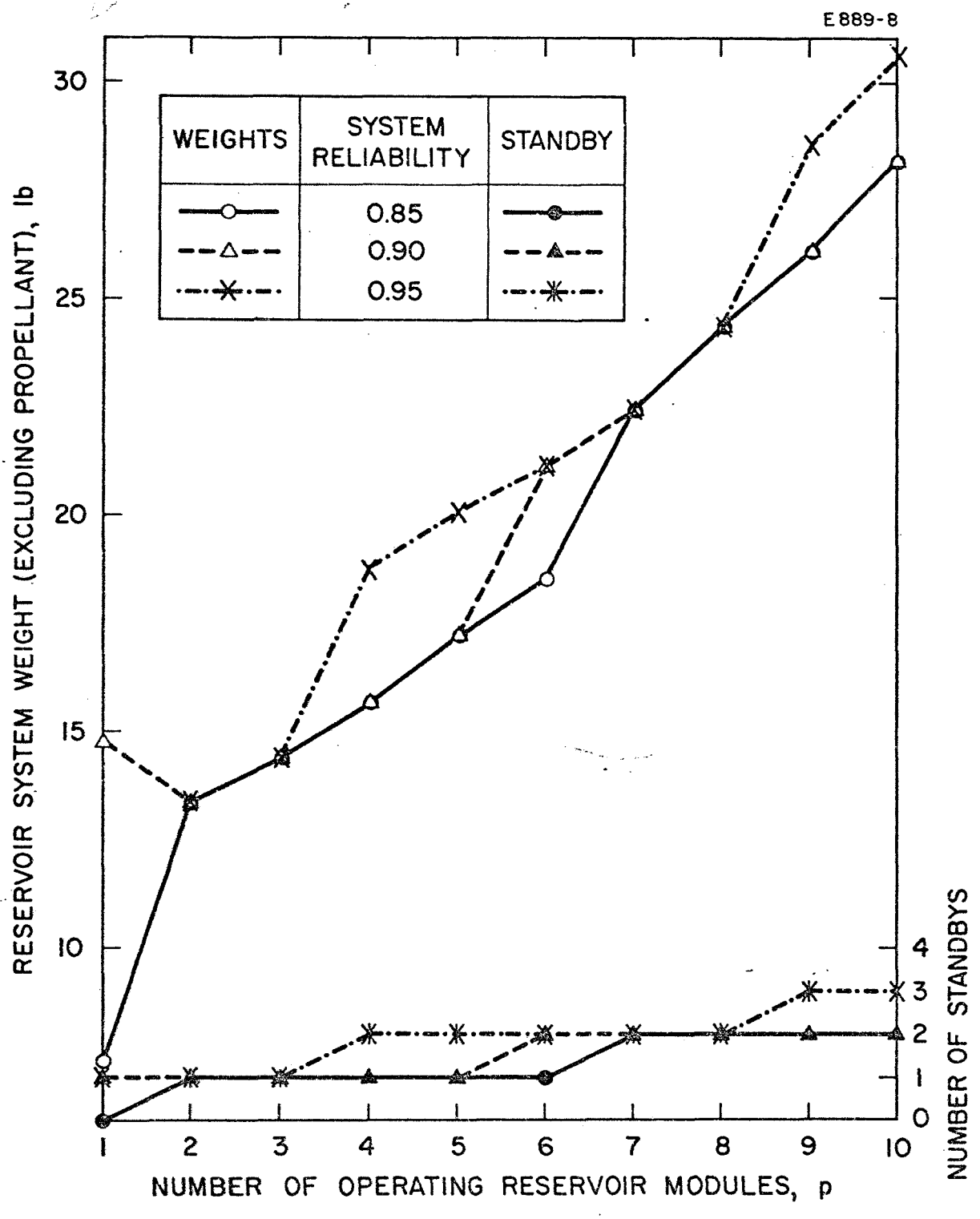

Fig. 10. Modularized reservoir system weight (assumes 865 lb of propellant, i.e., no propellant in standby tankage).

redundant propellant as well as tankage. Figure 11 shows the total weight of the reservoir system, including propellant, as a function of the degree of modularization employed and for over-all system reliabilities of 0.85, 0.90, and 0.95. This figure also shows the number of standby tanks required to raise the system reliability to the desired level. Again for $\overline{R} \geq 0.85$, the minimum system weight occurs when $p = 1$ and $q = 0$. However, for desired system reliabilities greater than 0.90 and 0.95, the optimum number of operating and standby tanks (p, q) is (5, 1) and (8, 2), respectively. In this case, the (5, 1) set provides a very small system reliability increase from 0.8988 (i.e., $p = 1$, $q = 0$) to 0.9105 at a weight penalty of 183 lb. In contrast, if the system reliability is increased to 0.9548 (i.e., $p = 8$, $q = 2$), the weight penalty is 233 lb.

The minimum system weight for various desired levels of system reliability is given in Fig. 12. This figure shows data for system designs where propellant is included in the redundant tankage and for designs where propellant is excluded. It should be noted that a relatively large weight penalty must result in both cases when the system reliability is increased from 0.89 to 0.90. However, once this initial step is taken in the system design, further reliability gains (e.g., up to 0.97) can be made with much less added weight increment.

The optimum number of initially operating reservoir modules, as well as the required number of standbys, is given in Fig. 13 as a function of over-all reservoir system reliability. The (p, q) pairs provided for each value of $\overline{R}$ are consistent with the system weights shown in Fig. 12. Since the reliability of a single large reservoir (liquid mercury capacity of 865 lb) is 0.8988, Fig. 13 shows that the minimum weight system for $\overline{R}$ values up to 0.90 consists of one operating tank and no standbys. (This situation is of course true for both the propellant included and propellant excluded cases.) For the system design where the propellant is included in the redundant tankage, the system reliability can be increased from 0.8988 to greater than 0.97 by employment of two operating reservoirs with one standby (i.e., $p = 2$, $q = 1$).

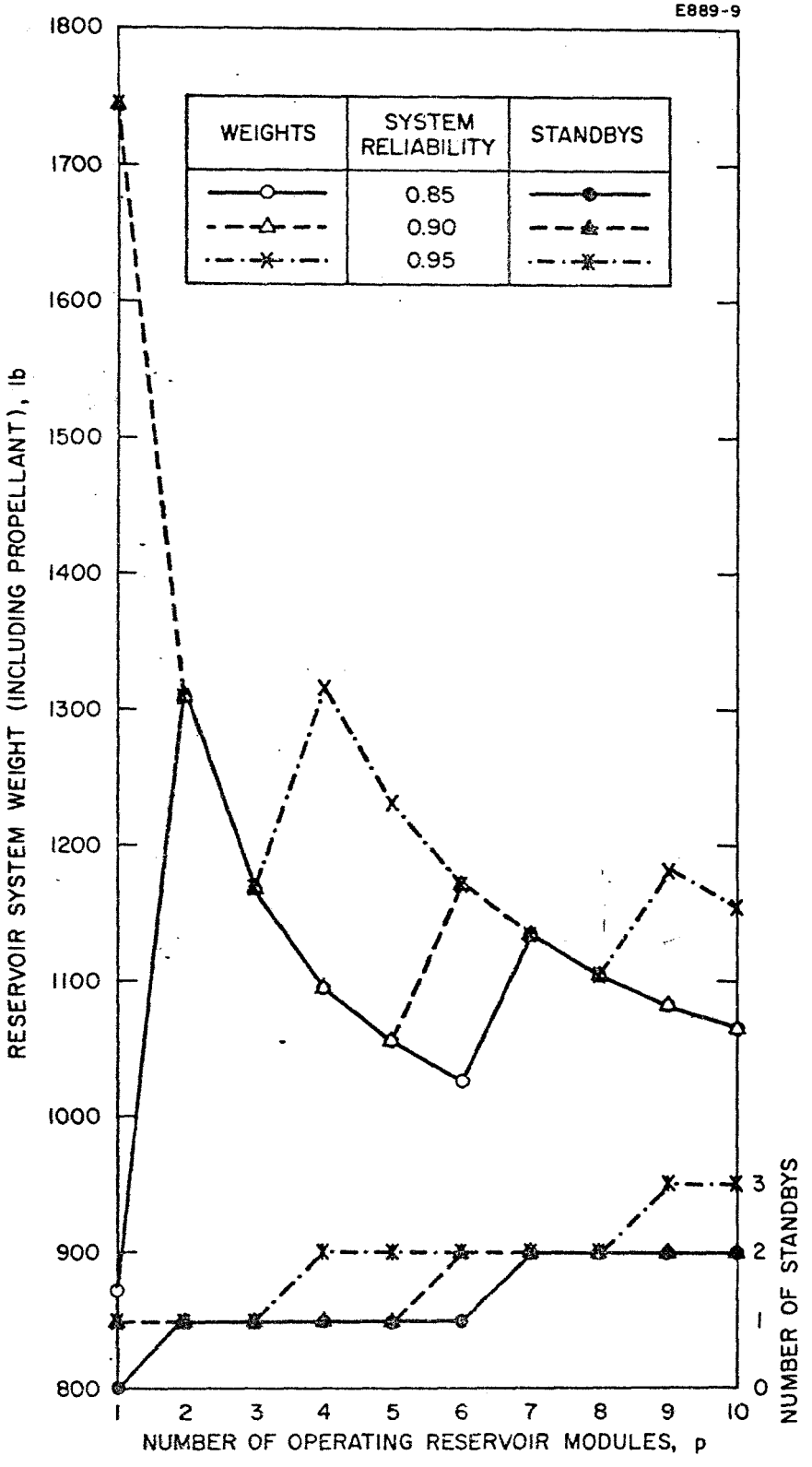

Fig. 11. Modularized reservoir system weight (assumes propellant in both operating and standby tankage).

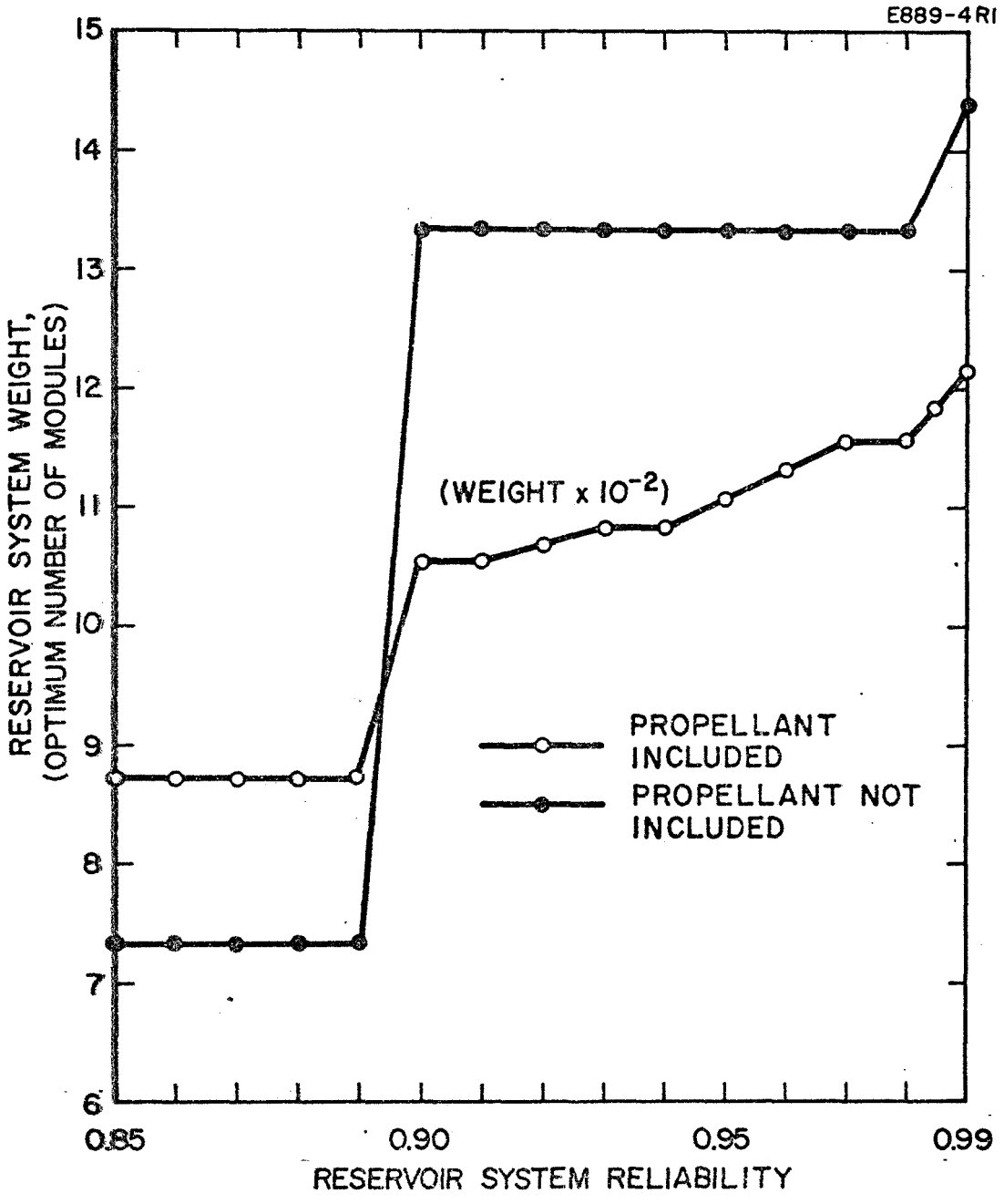

Fig. 12. Minimum reservoir system weight.

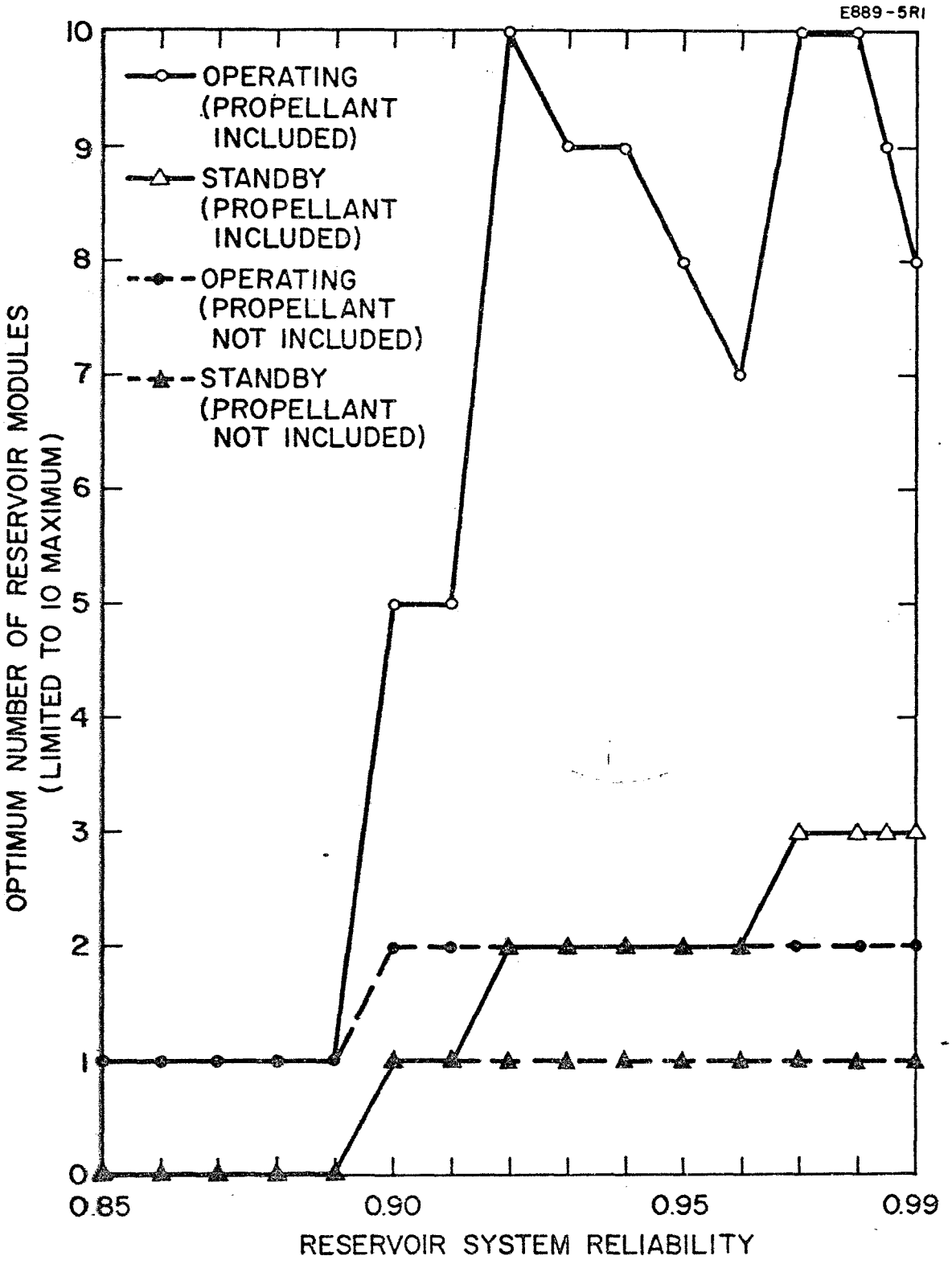

Fig. 13. Optimum number of reservoir modules required to obtain desired system reliability.

In the case where propellant is carried in the standby reservoirs, the optimum pairs of (p, q) vary considerably for desired system reliabilities in the 0.90 to 0.97 range.

b. Weight

The weight W_s of the Class 2 systems is given by

$$W_s = 8\,W_1 + 6\,W_2 + W_3 + (W_{p,q})_{opt} \tag{15}$$

where W_1, W_2, W_3, and $(W_{p,q})_{opt}$ are as defined previously.

3. Model No. 3

a. Reliability

Figure 2(c) shows that the Class 3 system configuration can be broken into three elements. The total system reliability is again given by the product of the reliabilities of these three elements. In terms of propulsion system components and subsystems, these elements consist of (1) the thruster array, valves, and EM pumps; (2) a common power conditioning unit; and (3) a reservoir system.

In this reference configuration redundancy is again provided in the thruster array. However, since no electrical isolation is provided, redundancy is ineffective in the event of certain types of thruster failures (e.g., shorts). Thus, the reliability of the first element is given by

$$R_1 = R_a \cdot R_b \tag{16}$$

where R_a is provided by the computer program described above. λ_a is defined as the effective failure rate of events which do not cause failure of the total system (e.g., opens), and R_b is given by

$$R_b = e^{-m_o \lambda_b \Delta t_1} \times e^{-(m_o - 1)\lambda_b \Delta t_2} \times \ldots \qquad (17)$$

$$R_b = e^{-\sum_{\mu=1}^{m_o} (m_o + 1 - \mu)\, \lambda_b \Delta t_\mu}$$

λ_b is the failure rate of events which cause total system failure, and Δt_μ represents the time intervals associated with the switching of thrusters as a result of solar panel power output variations.

In order that a fair comparison can be made between the decoupled and nondecoupled (i.e., reference) systems, it will be assumed that the six modularized power conditioning panels will be tied in parallel across the engine array load. Since thrusters will be turned off as the solar panel power output decreases, redundant power conditioning panels will become available as the mission proceeds. However, this redundancy is again ineffective against certain failure modes, so that the reliability R_2 of this element is

$$R_2 = R_c \cdot R_d \qquad (18)$$

where R_c is obtained with the computer program described above. λ_c is defined as the failure rate of events which do not cause total system failure, and R_d is given by

$$R_d = e^{-\sum_{\mu=1}^{m_o} (m_o + 1 - \mu)\, \lambda_d \Delta t_\mu} \qquad (19)$$

where λ_d is the failure rate of events which cause total system failure.

In order that a fair comparison may be made among system configurations, the reservoir system and manifold will be assumed identical to that provided for the Class 2 system; that is, R_3 and R_4 will have Class 2 values.

b. Weight

The weight W_s of the Class 3 system configuration is given by (15).

C. SYSTEM COMPARISON

Using the analytical models and parametric data developed in Section II-B, along with the component failure rates and weights provided in Appendix I, it is now possible to assess quantitatively the reliabilities and weights of the various system configurations shown in Fig. 1. Based on the failure rates listed in Appendix I, the reliabilities for 500 hour operation of the major system components have been determined and are given in Table I; the component weights are also summarized in this table.

TABLE I

Component Reliabilities and Weights

Component	Reliability	Weight, lb
Thruster	$R_t = 0.916$	$W_t = 10.86$
Insulating Valve (includes associated solenoid valve)	$R_{iv} = 0.956$	$W_{iv} = 0.25$
Solenoid Valve	$R_{sv} = 0.970$	$W_{sv} = 0.18$
EM pump	$R_p = 0.931$	$W_p = 0.64$
Isolator (bubble)	$R_i = 0.966$	$W_i = 0.82$
Manifold	$R_m = 0.994$	$W_m = 0.84$
Power Conditioning Panel[a]	$R_{pc} = 0.952$	$W_{pc} = 20.00$

[a] See Ref. 2

In order to evaluate the system reliabilities and weights, it is convenient to group the various configurations according to the appropriate analytical model.

1. Model No. 1

This first analytical model can be used to determine the reliabilities and weights of system configurations A-1, A-2, A-3, and C-2 shown in Fig. 1.

a. System Configuration A-1

In this configuration, a failed thruster can be isolated from the remaining operable thrusters by closing the insulating valve. However, all thrusters are electrically coupled during operation. An obvious disadvantage to this design is that all engines must be shut down and restarted if a trip occurs in any operating thruster.

Although each thruster operates from its own power conditioning panel, the high voltage beam supplies will be electrically coupled. For this reason, engine loads must be precisely matched. However, since this matching can be provided by the beam current-propellant flow control loop, no penalty in system reliability or weight will result.

Each thruster is provided with its own reservoir system. Propellant flow control is achieved through the positive expulsion system associated with the reservoir. Each reservoir (including standbys) is sized to contain 1/6 of the 865 lb of liquid mercury required to perform the mission. If a failure occurs in an engine or any associated component, its reservoir (and the remaining propellant) is lost. However, it is assumed that transfer of propellant from a reservoir associated with an engine which has been switched off because of a decrease in available power to an operating engine can be accomplished with no penalty to system reliability or weight.

The first element (e.g., see Fig. 2) of the analytical model for this configuration consists of six initially operating and two standby groupings of components which include a thruster, insulating valve,

reservoir (144 lb liquid mercury capacity), and a solenoid valve. The reliability R_g of this grouping is $R_g = R_t \cdot R_{iv} \cdot R_r \cdot R_{sv}$. The values of R_t, R_{iv}, R_{sv} are found in Table I, and R_r (the reservoir reliability) can be obtained from the failure rate data in Fig. 8. Thus, $R_g = 0.770$. The reliability R_1 of the first element is found from Fig. 4 to be $R_1 = 0.980$.

The reliability R_2 of the second element (i.e., the complete power conditioning and control system) which can be obtained from Fig. 5 using a single panel reliability of 0.952 is found to be 0.906.

The third element, or manifold, reliability R_3, as well as all component weights, can be obtained directly from Table I. Thus, the total system reliability and weight for the A-1 configuration is

$$\begin{aligned} R_s &= R_1 \cdot R_2 \cdot R_3 \\ &= 0.980 \times 0.906 \times 0.994 \\ &\cong 0.88 \end{aligned}$$

and

$$\begin{aligned} W_s &= 8\,W_1 + 6\,W_2 + W_3 \\ &= 8\,(W_t + W_{iv} + W_r + W_{sv}) + 6\,W_{pc} + W_m \\ &= 8\,(10.86 \text{ lb} + 0.25 \text{ lb} + 2.70 \text{ lb} + 0.18 \text{ lb}) \\ &\quad + 6(20.00 \text{ lb}) + 0.84 \text{ lb} \\ &\cong 233 \text{ lb} \end{aligned}$$

The propellant weight for this system is 1153 lb (i.e., eight reservoirs each containing ~144 lb of mercury).

b. System Configuration A-2

The reliability R_2 and weight W_s of system configuration A-2 are identical to those of A-1. The one major advantage of A-2 over A-1 is that all engines are electrically decoupled during operation.

c. System Configuration A-3

Configuration A-3 provides electrical isolation between operating engines. In addition, if desired, a failed thruster can be separated from its reservoir. The difference in system reliability R_s and weight W_s between configuration A-3 and A-1 (or A-2) is simply the substitution of an insulating valve for the solenoid valve. Making this numerical substitution yields

$$R_s \cong 0.88$$

$$W_s \cong 233 \text{ lb} \quad .$$

The weight of the propellant is again 1153 lb.

d. System Configuration C-2

Configuration C-2 makes use of an isolator component between each thruster and its reservoir. This system design provides for isolation between operating thrusters and between thruster array and tankage system. Although thruster array and tankage are at all times completely decoupled electrically in configuration C-2, a reservoir is provided for each thruster. Thus, propellant flow control can be achieved by means of a control loop between the thruster beam current and the positive expulsion system of its associated reservoir. The reliability of the thruster plus related components such as isolator, two solenoid valves, and reservoir is

$$R_g = R_t \cdot R_i \cdot R_{sv} \cdot R_r \cdot R_{sv}$$

$$R_g = 0.753 \quad .$$

The first element reliability R_1 for this configuration is seen from Fig. 4 to be $R_1 = 0.975$. Since R_2 and R_3 are identical to configuration A-1, the total system reliability R_s is

$$R_s = 0.975 \times 0.906 \times 0.994$$

$$\cong 0.88 \ .$$

The total system weight W_s is given by

$$W_s = 8 (W_t + W_i + 2W_{sv} + W_r) + 6 W_{pc} + W_m \ .$$

$$= 8 (10.86 \text{ lb} + 0.82 \text{ lb} + 0.36 \text{ lb} + 2.70 \text{ lb}) + 6 (20.00 \text{ lb}) + 0.84 \text{ lb}$$

$$\cong 239 \text{ lb}.$$

As in the previous configurations, the propellant weight is 1153 lb.

2. Model No. 2

The second analytical model describes the reliabilities and weights of system configurations B-1, B-2, and C-1.

a. System Configuration B-1

In configuration B-1 the reservoir subsystem can be designed (i.e., the number of reservoirs chosen) independently of thruster array considerations. Thus, the tankage system can be optimized so that a minimum system weight results for a given desired reliability. In this configuration the reservoir system is common to the total thruster array; therefore, propellant flow control to an individual engine is provided by an electromagnetic pump. As in configurations A-1, thrusters are electrically coupled while they are operating. However, if an engine fails, it can be isolated from the rest of the system by closing the insulating valve in the feed line. In addition, as in A-1, the operating ion engine loads are properly balanced by means of the beam current-propellant flow control loop.

The first element of the analytical model again consists of six operating and two standby groupings of components, including thruster, electromagnetic pump, and insulating valve. The reliability of this component grouping is $R_g = R_t \cdot R_p \cdot R_{iv}$. From the data in Table I, R_g is found to be 0.813, resulting in a reliability R_1 of 0.990 for the first element. The reliabilities of the second and third elements are, as before, 0.906 and 0.994, respectively.

Since the reliability R_4 of the fourth element (the reservoir system) can be chosen independently, some criterion for the choice must be established. For the sake of comparison, the reliability R_4 will be chosen such that the weight of configuration B-1 is equal to that of A-1. The total weight of system A-1, including propellant, is 1386 lb. The weight of configuration B-1 is $W_s = 8\,(W_t + W_p + W_{iv}) + 6\,W_{pc} + W_m + W_{rs}$. Here W_{rs} is the weight of the reservoir system including propellant. Thus, for the comparison, let $W_s = 8$ (10.86 lb + 0.64 lb + 0.25 lb) + 6 (20.00 lb) + 0.84 lb + W_{rs} = 1386 lb, yielding W_{rs} = 1171 lb. The reliability $\bar{R}$ of an optimized reservoir system of this weight is (from Fig. 12) greater than 0.98 (actually 0.988). Figure 13 shows that this system would consist of nine operating and three standby reservoirs.

The total system reliability R_s for this configuration (allowing a total system weight W_s, including propellant, of 1386 lb) is then

$$\begin{aligned} R_s &= R_1 \cdot R_2 \cdot R_3 \cdot R_4 \\ &= 0.990 \times 0.906 \times 0.994 \times 0.988 \\ &\cong 0.88 \ . \end{aligned}$$

Thus, for an equal system weight condition, the reliability of configuration B-1 is equivalent to the systems A-1, A-2, and A-3.

b. System Configuration B-2

Except for the substitution of a small reservoir and solenoid valve for the EM pump, configuration B-2 is similar to B-1. However, a more complex operational procedure is required in B-2. Although the main reservoir system design is independent, a small reservoir is provided for each thruster. Propellant flow control is accomplished by means of a control loop between the beam current and the positive expulsion system of the small reservoir. During normal operation all insulating valves are closed, providing electrical isolation between individual thrusters and the thruster array and tankage. In the event of failure of a thruster (or any component duplicated with each thruster), isolation from the remaining thrusters is maintained by the insulating valve. Each thruster is operated from the propellant in its associated small reservoir. Each time these reservoirs are emptied, the propulsion system must be shut down, the insulating valves opened, the solenoid valves closed, and the small reservoirs refilled. Although the size of the small reservoir is open to choice, it must be relatively small (e.g., 10 lb liquid mercury capacity) to make the system concept different from configuration A-2. The weight W_r' of a 10 lb liquid mercury capacity reservoir is 2 lb (extrapolating the data in Fig. 6).

Using the same criterion of equal system weight to establish a reliability comparison among the various configurations, the weight of system B-2 is expressed by

$$W_s = 8(W_t + W_{sv} + W_r' + W_{iv}) + 6\,W_{pc} + W_m + W_{rs}$$
$$= 1386 \text{ lb}$$

$$= 8\,(10.86 \text{ lb} + 0.18 \text{ lb} + 2.00 \text{ lb} + 0.25 \text{ lb}) + 6\,(20.00 \text{ lb}) + 0.84 \text{ lb} + W_{rs} + 1386 \text{ lb}\ ,$$

giving a main reservoir system weight of $W_{rs} = 1159$ lb. The reliability $\overline{R}$ of the optimum reservoir system of this weight is 0.983, with ten operating tanks and three standbys.

The thruster group reliability R_g for B-2 is

$$R_g = R_t \cdot R_{sv} \cdot R_r' \cdot R_{iv}$$
$$= 0.916 \times 0.970 \times 0.909 \times 0.956$$
$$= 0.772 \ .$$

From Fig. 4, the reliability R_1 of the first element is 0.980, giving a total system reliability

$$R_s = R_1 \cdot R_2 \cdot R_3 \cdot R_4$$
$$= 0.980 \times 0.906 \times 0.994 \times 0.983$$
$$\cong 0.87$$

c. System Configuration C-1

System configuration C-1 employs an isolator component in the propellant feed line of each thruster. The isolator provides total electrical decoupling between individual thrusters, between power conditioning systems, and between the reservoir system and the thruster array and power conditioning units. Furthermore, this isolation is provided while engines are operating; therefore, a trip in one engine or power conditioner is not reflected in the remaining units. All engines receive propellant from a common manifold, and flow to an individual thruster is controlled by means of an electromagnetic pump. The reservoir system of course can be designed (i.e., in terms of number of tanks) to be independent of other major subsystems, and no propellant transfer from tank to tank is required. Thus, the C-1 configuration accomplishes complete and continuous electrical isolation between all subsystems, with none of the undesirable operational procedures required by the previous configurations.

The thruster grouping for this design consists of a thruster, EM pump, isolator, and solenoid valve. The reliability of this group is

$$R_g = R_t \cdot R_p \cdot R_i \cdot R_{sv}$$
$$= 0.916 \times 0.931 \times 0.966 \times 0.970$$
$$\cong 0.80 \ .$$

The reliability R_1 of the first element is, from Fig. 4, 0.988. The reliabilities of the second and third elements are 0.906 and 0.994, respectively. As before, the reservoir reliability R_4 is determined by choosing a total system weight equal to the weight of configuration A-1. Thus, $W_s = 8\,(W_t + W_p + W_i + W_{sv}) + 6\,(W_{pc}) + W_m + W_{rs}$ = 1386 lb, which gives an allowed reservoir system weight, including propellant, of W_{rs} = 1165 lb. The reliability of a reservoir system which weighs 1165 lb and consists of the optimum combination of operating and standby tanks (i.e., p = 9, g = 3) is, from Fig. 12, 0.988. The total system reliability is then

$$R_s = R_1 \cdot R_2 \cdot R_3 \cdot R_4$$
$$= 0.988 \times 0.906 \times 0.994 \times 0.988$$
$$\cong 0.88 \ .$$

From these results, it is apparent that the reliabilities and weights of all the isolation schemes (i.e., system configurations) studied are approximately equal. Therefore, the final choice of design must be made on the basis of (1) degree of isolation provided, (2) operational simplicity, and (3) availability of components. In each of these three areas, configuration C-1 is substantially superior to the others.

3. Model No. 3

The third analytical model describes the reliability and weight of the reference system (configuration D-1) for this study. The reference system contains no electrical isolation. The six power conditioning panels are hooked in parallel across the thruster array load. In this system design, a trip in any individual engine requires shutdown and restart of all operating engines in the array. It is assumed that any thruster or power conditioning panel which has been shut down because of a decrease in available power can be reinstated to replace a failed unit.

In order to determine the reliability R_1 of the first element of this nondecoupled system, the failure modes of the thruster must be divided into two categories: those which are covered by the redundant engine systems and those which cause catastrophic failure of the complete system. Table II lists the possible failure modes of a liquid mercury cathode electron-bombardment ion engine, indicating the failures which affect only the individual engine and those which are reflected through the complete system.

TABLE II

Thruster Failure Modes

Component	Effect of Failure	
	Single Thruster	Complete System
Cathode	X	
Neutralizer	X	
Vaporizer	X	
Magnet	X	
Electrodes	X	X
Insulators	X	X
Connectors	X	X

Using the thruster component breakdown in Appendix I, it is now possible to determine the total failure rate associated with a catastrophic system failure λ_b (see items in Appendix I with asterisk), as well as the total failure rate related to a single thruster λ_d. Using a λ_d value of 6.54×10^{-6} failure/hour, the reliability R_t of a thruster (neglecting failures catastrophic to the system) is 0.924. Therefore, the reliability of the thruster group is

$$\begin{aligned} R_g &= R_t \cdot R_p \cdot R_{sv} \\ &= 0.924 \times 0.931 \times 0.970 \\ &= 0.834. \end{aligned}$$

From Fig. 4 the reliability R_d of that part of the first element (e.g., see Fig. 2(c)) of configuration D-1 is 0.994. The value of λ_b is estimated to be 0.796×10^{-6} failures/hour. From (17), R_b is 0.968, and the reliability of the first element is

$$\begin{aligned} R_1 &= R_d \cdot R_b \\ &= 0.962 \quad . \end{aligned}$$

A similar type of analysis must now be made to determine the reliability R_2 of the second element (i.e., power conditioning system). Reference 2 describes the failure modes associated with a modularized power conditioning system. Using the results of the analysis in Ref. 2, the individual power supply failures which would affect total propulsion system failure, as well as estimates of the probability that these failures would <u>not</u> occur, are presented in Table II.

The reliability R_{pc} of the power conditioning system, excluding the catastrophic failures listed above, can be shown to be 0.972 (compared with the 0.952 shown in Table I). The value of R_c (see Fig. 2(c)) is then shown by Fig. 5 to be 0.945. From the data in Table III the effective failure rate λ_d of catastrophic power conditioner failures is found to be 1.725×10^{-6} failures/hour. Substituting this value into (19), the value of R_d becomes 0.931. The reliability of the second element is then

TABLE III

Catastrophic Power Conditioner Failure Modes

Supply	Component Failure Modes	Associated Reliability
Beam	High Voltage Filter (any component)	0.9974
	High Voltage Transformer (insulation)	0.9982
	Series String Connectors (short to ground)	0.9975
Heater Inverter and Switching Circuit	Low Voltage Rectifier (short) or Filter (short to ground)	0.9984
Cathode	Input Transformer (short or short to ground)	0.9996
Discharge	Input Transformer (short to ground)	0.9994
	Output Transformer (short to ground or open secondary)	0.9998
Accelerator	High Voltage Filter (any component)	0.9986
	External Connectors (short to ground)	0.9999

$$R_2 = R_c \cdot R_d$$
$$= 0.945 \times 0.931$$
$$= 0.880 .$$

As with all system configurations, the manifold reliability is 0.994.

Since the degree of reservoir modularization in the nondecoupled reference system is independent of other subsystems, an equal weight criterion will again be used. The weight of the total system is $W_s = 8 (W_t + W_p + W_{sv}) + 6 W_{pc} + W_m + W_{rs} = 1386$ lb. Substituting the component weights from Table I, the allowed reservoir system weight is 1172 lb. Figure 12 shows that a system design with nine operating and three standbys provides the highest system reliability (i.e., $R_4 = 0.988$) for this weight.

The reliability of the reference system is then

$$R_s = R_1 \cdot R_2 \cdot R_3 \cdot R_4$$
$$= 0.962 \times 0.880 \times 0.994 \times 0.988$$
$$\cong 0.83 .$$

These results show that the reliability of systems with some isolation scheme is somewhat greater (e.g., 0.88 compared with 0.83) than that of the completely nondecoupled system (assuming equal system weights). However, as was pointed out earlier, an equally important consideration in comparing systems is the operational characteristics of the configuration. On that basis, the nondecoupled system becomes even less desirable than the most attractive decoupled system (configuration C-1).

SECTION III

COMPONENT DEVELOPMENT

A. ELECTRICAL ISOLATOR CONCEPTS

Because a liquid mercury column is a good electrical conductor, it is immediately apparent that any type of electrical isolator must provide a means for mechanically interrupting this column. The several possibilities available for accomplishing this interruption are the use of a solid, liquid, or gaseous material inserted in the mercury propellant feed line. These techniques will be discussed below.

1. Solid Electrical Interrupter

Conceptually, solid devices may consist of rotating vanes ("Roots Blower") or a close fitting pair of gears fabricated from insulating material placed in the propellant line. A second technique would be to use a single gear in a close fitting housing, which carries mercury between the gear teeth to the downstream side, where it is forced out by an idler gear (Fig. 14). Unsuccessful attempts[4] have been made with similar techniques, and no design improvements have been developed which would eliminate the basic problem of the required close mechanical tolerances of the gears. Fundamentally, the problem is that very close tolerances between mechanical components are required to assure that a mercury film is not left on a surface which must provide electrical insulation. It is difficult to maintain these tolerances over many thousands of hours of operation.

It was concluded that a major effort would be required to reduce to practice one of the above two designs, and that the component reliability would be questionable at best.

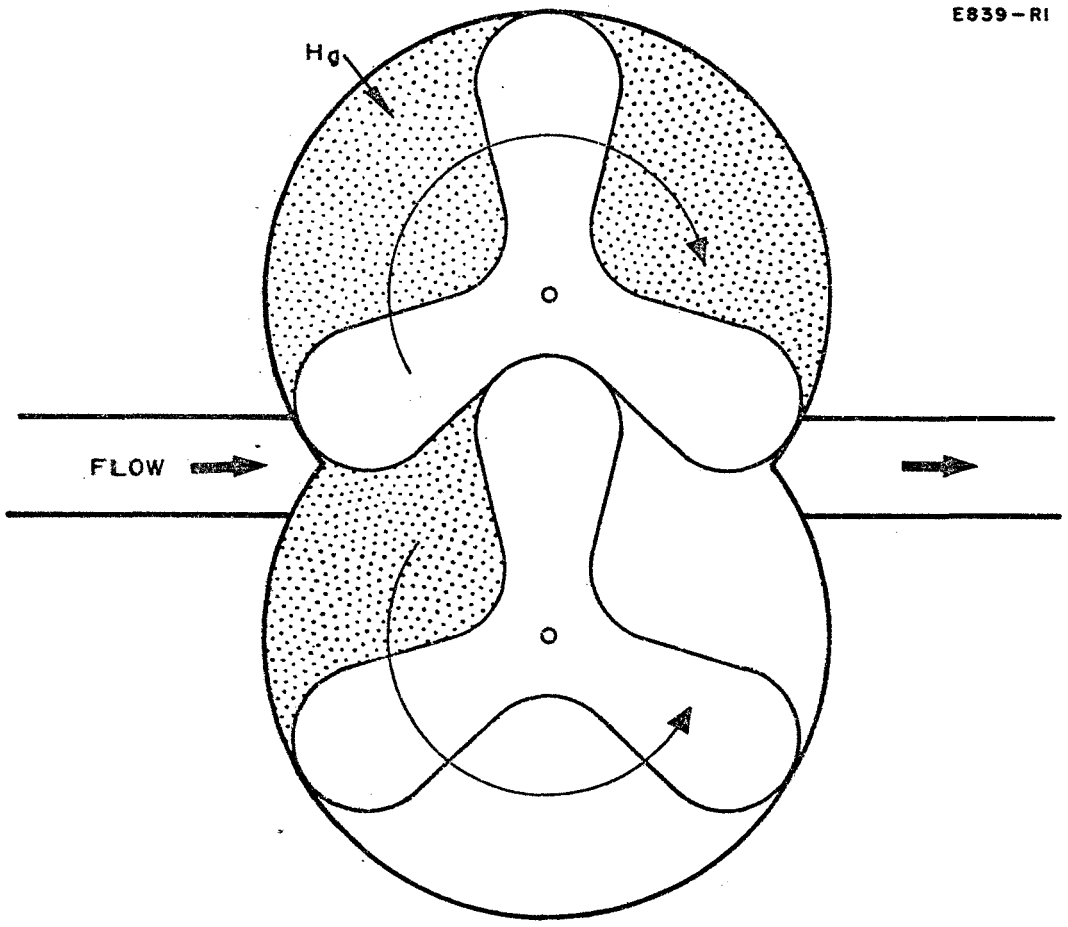

(a)

Fig. 14. Conceptual gear type isolators.

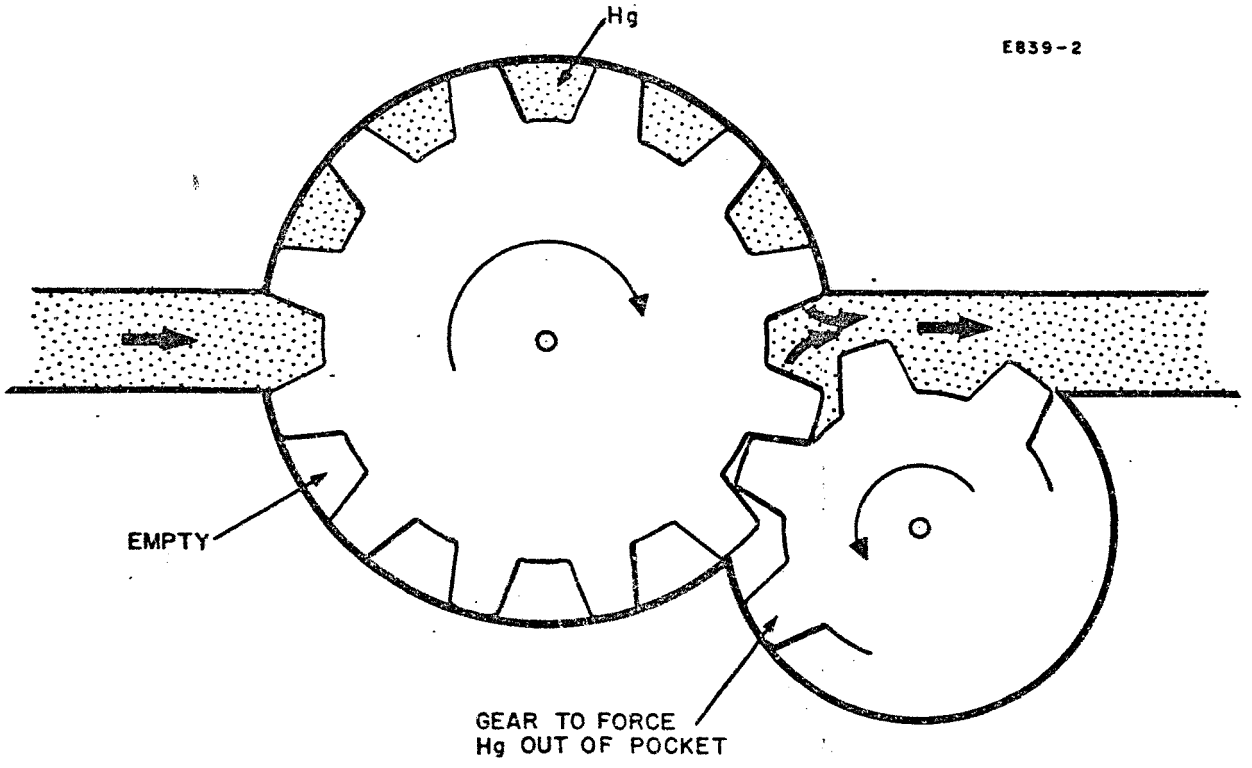

(b)

Fig. 14. Conceptual gear type isolators.

2. Liquid Electrical Interrupter

No satisfactory designs using a liquid were discovered or developed.

3. Gaseous Interrupter

The gaseous technique appears to be the most promising. Two potentially useful designs were evolved. The first consists of converting the liquid mercury to a vapor in an insulating section of the propellant line and adjusting the product of the pressure times the gap spacing to assure that electrical breakdown will not occur. This technique has been demonstrated at HRL for vapor fed thermionic and hollow cathode mercury thrusters operating at propellant line pressures up to 50 Torr. Such a device is conceptually simple and passive. In order to apply this same concept to a liquid mercury propellant system, a condenser is required on the downstream side of the isolator. While it was felt that such a system was possible, two major problems exist. The first was one of materials compatibility. Liquid mercury cathodes require propellant line pressures of >30 psi for satisfactory operation. Thus, the vapor section of the propellant line must operate at temperatures greater than $400^{\circ}C$ to prevent condensation. Such high temperature operation accelerates the mercury corrosion of the propellant line components, particularly the braze material used to fabricate the ceramic-to-metal joints. The other problem is associated with the dynamic response of the system, especially during startup. The technical problems associated with this type of device are in the generation and subsequent condensation of the vapor at the low temperature end of the isolator section. Although both difficulties appear solvable, they were considered disadvantages when compared with the more simple approach described below.

The electrical isolator design selected involves the injection of a bubble of suitable gas into a narrow column of liquid mercury as it flows through an insulating section of the propellant line. The insulating properties of the gas column are described (approximately for this

geometry) by the Paschen electrical breakdown curves[5, 6] for the particular gas chosen. The Paschen curves define the maximum potential which can be applied across a length of gas d at a particular gas pressure p. For the pressures of interest, spacings of a few millimeters can stand off several kilovolts. Such an isolator system is shown in Fig. 15. The figure also shows a porous section of line downstream of the isolator from which the gas is able to escape into the vacuum while the liquid mercury propellant travels on to the cathode.

B. ELECTRICAL ISOLATOR DESIGN

1. Basic Configuration

The basic concept of electrical isolation provided by a gas bubble in an insulating section of line, and the reasons for choosing it over competing methods, were discussed above. The factors involved in implementing this design as functional hardware are discussed below. They include the techniques by which gas bubbles are to be controlled in size and injected into the propellant line, the size of the various components, the materials to be used, the sensor to determine when a bubble has traversed the line and a new one is required, and the means of removing the gas bubble from the line and leaving the liquid mercury behind.

The bubble injection system is the most complicated. The basic requirement is that it inject gas bubbles of approximately 2×10^{-3} cm^3 volume at 30 psi into the line upon demand (at approximately 20 min intervals). Originally, it was proposed that this be done with a regulator and solenoid valving system of commercially available design. At the start of this program, specifications were sent to 22 valve and regulator manufacturers throughout the United States. Only the original vendor contacted during preparation of the proposal considered such a unit within the current state of the art and was prepared to supply such a device on a 120 day delivery schedule. After consultation with the JPL program monitor, this approach was abandoned in favor of the concept discussed below.

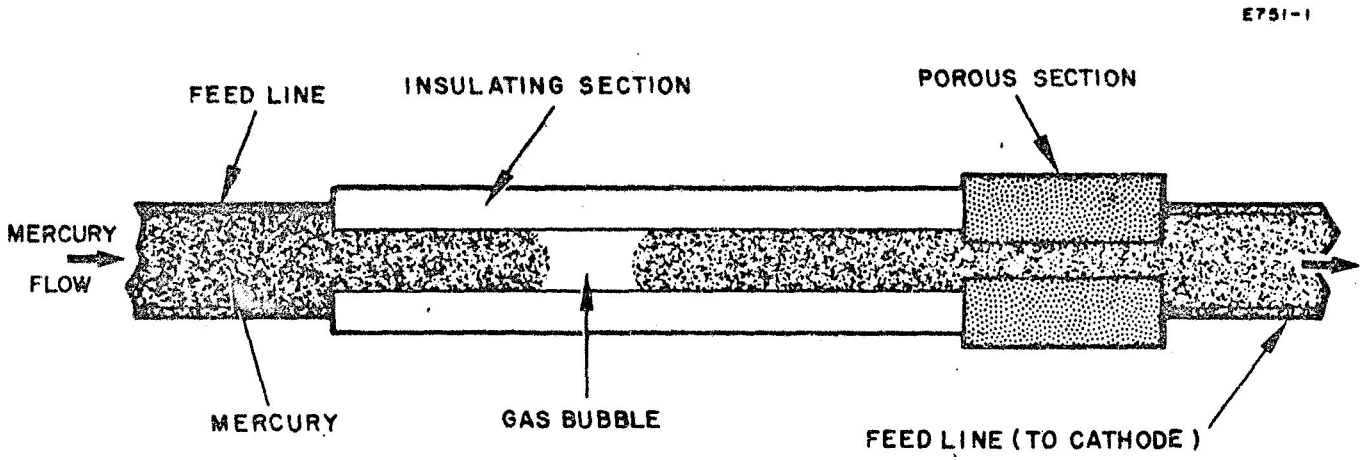

Fig. 15. Gas bubble isolator.

While vendors were replying to the request for quotation on the valve and regulator, other techniques for bubble injection were considered. The most promising of these was that a very slow leak from a high pressure gas source might serve the purpose and require no moving parts.[7] Based on this concept, the following bubble injection system was developed (see Fig. 16). High pressure hydrogen is stored in a small reservoir (~25 cm^3) which has an iron plug welded into the outlet line. By adjusting the temperature of the plug, the rate at which hydrogen diffuses through the iron may be controlled.* The hydrogen is collected in a small (< 1 cm^3) plenum downstream of the plug. When a gas bubble is required, this plenum is heated and the gas expands through a small diameter tube which pierces the propellant line wall just upstream of the electrical insulating section. With the temperature of the iron plug controlled, a gas bubble of any size may be created in the propellant line. The rate of temperature rise of the plenum controls the rate at which the gas expands, and thus the rate at which the bubble is formed. While a ball check valve could be inserted in the gas line to prevent mercury from entering the line when the plenum is cooled, in this design the line was sized so that it simply accommodated the mercury drawn into the line by the cooling gas. This mercury is later pushed out as the next bubble is formed.

A system must be developed to assure that bubbles are generated at the proper intervals to provide discontinuity in the mercury flow. The possible systems evaluated included integration of the mercury mass flow or ion beam current, variation in light transmission through a section of the column as it is occupied by the mercury and then a gas bubble, monitoring the resistance of a section of line with a pair of electrodes which pierce the insulating wall, capacitive and

*In a manner analogous to the more common hydrogen-palladium system.

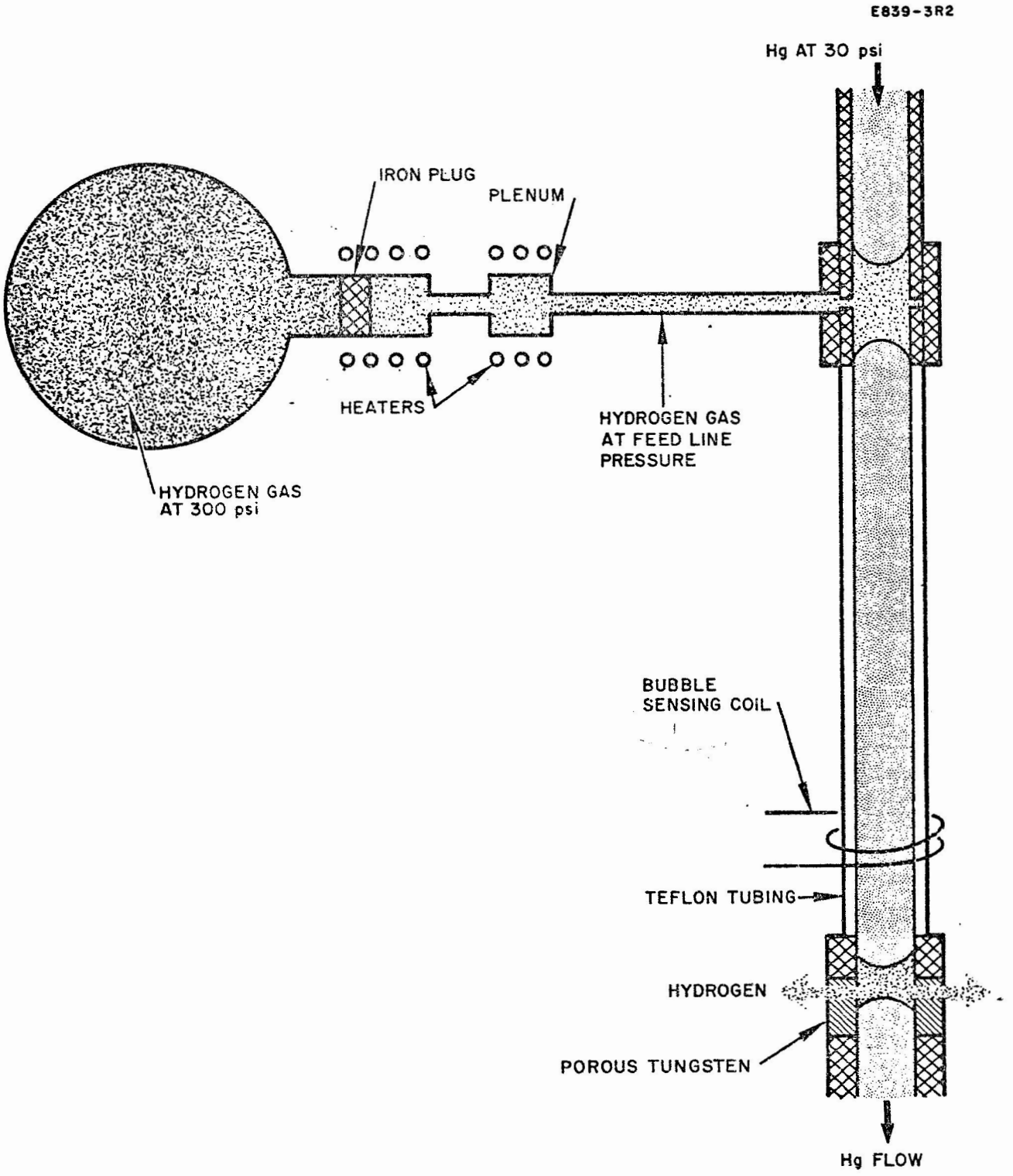

Fig. 16. Schematic of final isolator design.

inductive variations to an external electrode surrounding the insulating sections, or a simple timer which injects bubbles at a preset interval (which may depend on ion beam current). Of all sensing systems considered, the timer and the inductive coupling were found to be the best. The inductive system was chosen because it represented a closed loop design.

Design of the remainder of the bubble injection system was straightforward and involved choosing materials for the various components based on past experience and a knowledge of the wetting and corrosive properties of mercury. A molybdenum-rhenium alloy was used for the terminations of the insulating section because it is relatively ductile and is not attacked by mercury. A fine porous tungsten cylinder (manufactured at HRL) was used to vent the gas while holding back the liquid mercury. Double-walled teflon tubing serves as the electrical insulating section. This tubing may be coiled in the final design and reinforced with a glass filled teflon tubing if operation at high pressure is required. All metal-to-metal connections are electron beam welded; the teflon-metal connections are made mechanically strong with crimped bands, and can be sealed with epoxy if necessary.

2. Bubble Sensor

Based on the inductive coupling technique discussed previously, a gas bubble sensor was designed and tested. It consists of a small coil wrapped around the downstream end of the insulating section of line. This coil in parallel with a capacitor constitutes the tank circuit of a tuned crystal oscillator. As the bubble moves into the coil (thus replacing the mercury), the self inductance decreases and the output of the oscillator also decreases. This signal is rectified, and the dc voltage is used to turn on the plenum heater and produce the next gas pulse. A very desirable feature of this technique is that the sensor may remain at ground potential even though the dc potential of the mercury in the column varies by several thousand volts, thus obviating the need for isolation transformers.

3. Confirming Experiments

Before the final design could be completed, it was necessary to know accurately both the voltage breakdown characteristics for the particular geometry to be used (i.e., hydrogen bubble between mercury electrodes in a teflon tube) and the rate at which hydrogen gas diffused through an iron plug as a function of temperature. The importance of these two factors to the final design made it desirable to measure them experimentally to confirm the data in the literature before the design could be finalized.

a. Voltage Breakdown Measurements

Figure 17 shows published Paschen curves for mercury and for hydrogen taken under ideal conditions with large flat electrodes in a carefully designed tube. To confirm these data in the geometries of interest here, the following experiments were performed. A hydrogen bubble was trapped in a column of mercury in a glass tube with 0.075 cm internal diameter. A power supply in series with a $10^7\ \Omega$ resistor was connected across the gas bubble and the potential was increased slowly. The breakdown potential was determined easily by monitoring the current flowing in the power supply circuit. This potential, when plotted against the product of pressure times length of the bubble, is shown in Fig. 17. Later experimental data obtained with a teflon tube of the type used in the final hardware are also shown.

The published mercury Paschen electrical breakdown curve is shown in Ref. 5. It lies above the hydrogen curve and has no appreciable effect on the volume breakdown in the gap, especially since the anticipated operating temperatures are such that the mercury vapor pressure is less than 10^{-2} Torr.

A more serious problem encountered in these early experiments was that the mercury would appear to wet the teflon tubing periodically, bridging the bubble and causing a short circuit. A number of surface treatments were tried, as was a change from TFE teflon to FEP teflon. FEP teflon is extruded from the melt, and therefore has a smoother

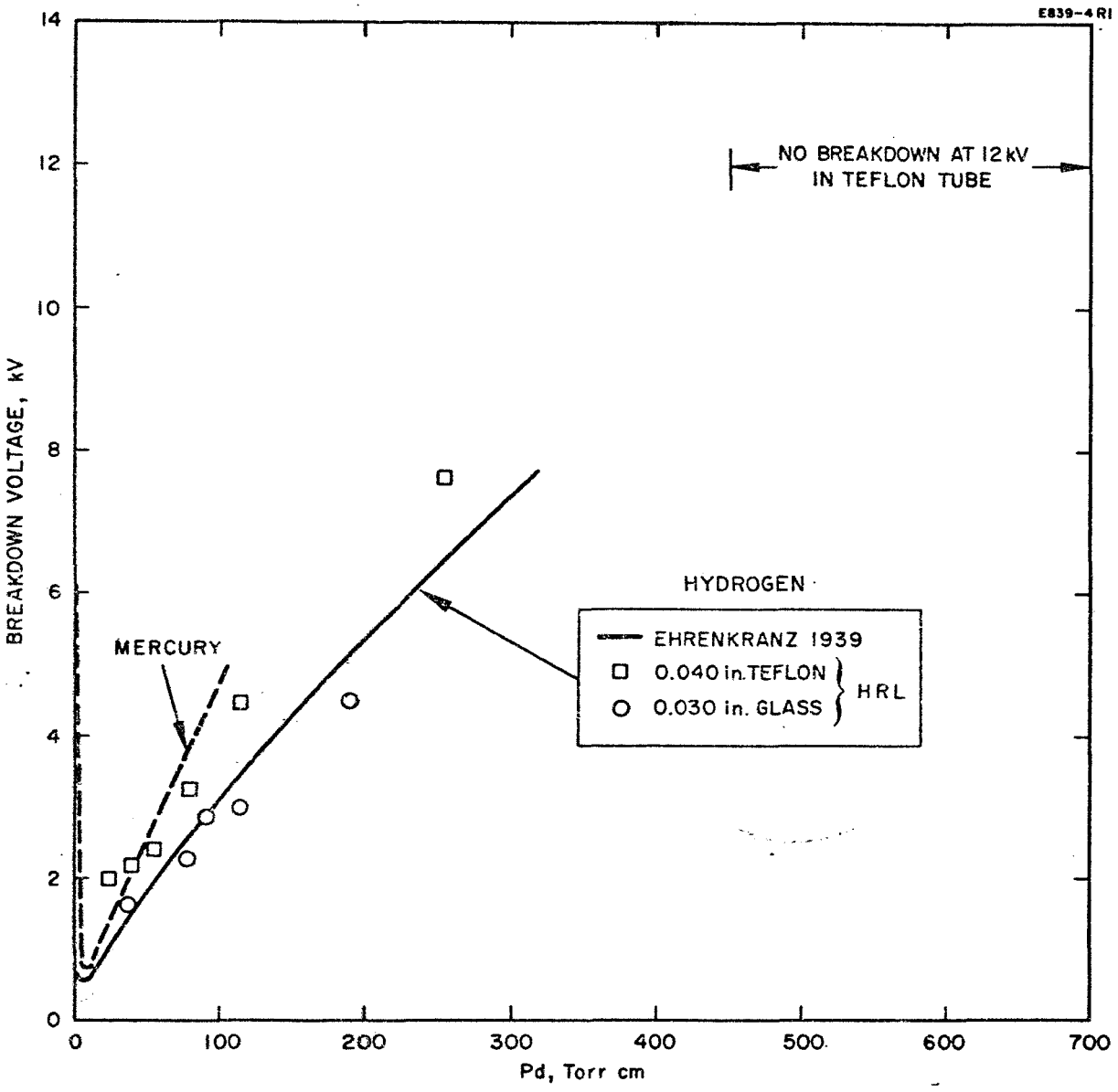

Fig. 17. Hydrogen diffusion through iron as a function of temperature.

surface finish than the TFE material. It was ultimately determined that this bridging occurred only when one end of the column was electrically isolated by the bubble; it appeared to be caused by an electrostatic surface charging of the teflon as the mercury passed over the surface. This problem has not occurred in several hundred hours of testing in the isolator, where both sides of the mercury column are electrically connected (though not to the same potential).

b. Diffusion of Hydrogen through Iron

A number of gas-metal combinations are potentially possible for the high pressure gas leak. The available data for several of the better known materials and a brief discussion of the diffusion mechanism are presented by Dushman.[8] The hydrogen-palladium system has the highest diffusion coefficient; however, little is known concerning the chemical interaction between mercury and palladium. Calculations based on Duschman's published constants indicated that the hydrogen-iron combination gave very reasonable design values (~250°C, 1 cm^2 area) for the flow rates desired.

Figure 18 presents data taken at HRL in confirmation of the published values of Smithells[9] for hydrogen through iron. The variation by a factor of 2 is unexplained, but it is of little consequence because of the exponential nature of the diffusion rate versus temperature.

4. Final System

With the data available from the above experiments, the final system design parameters may be determined.

a. Specifications

It was agreed with the JPL program manager at the onset of the program that the electrical isolator system would be designed for an ion thruster producing 1 A of ion beam current for 10^4 hours. This corresponds to a volume flow rate of 0.6 cm^3/hour if 80% propellant utilization in the thruster is assumed.

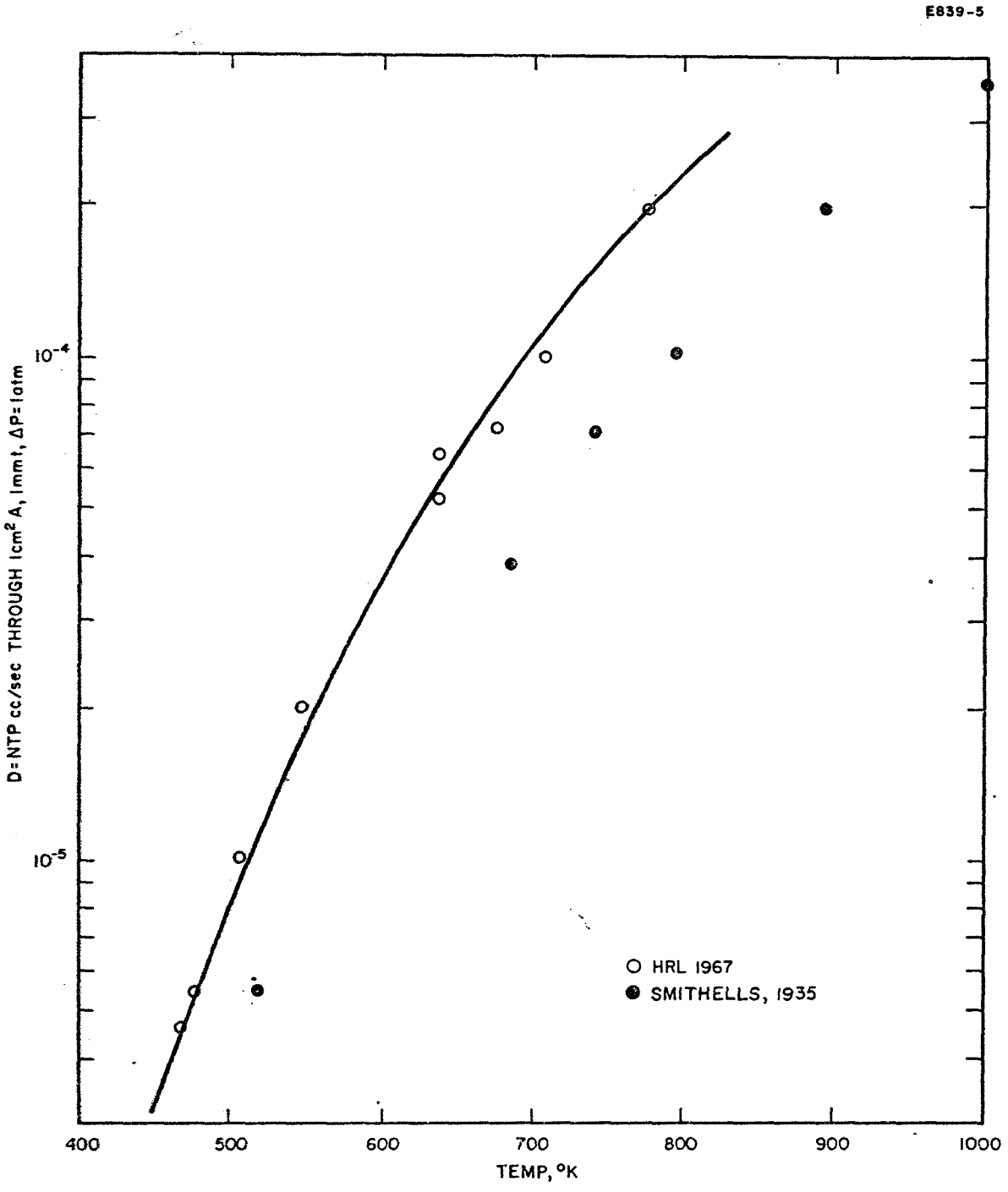

Fig. 18. Hydrogen diffusion through iron as a function of temperature.

Previous laboratory experiments at HRL defined that the liquid mercury cathodes require a propellant line pressure of ~1500 Torr or greater.

b. Design

(1) Thermal-Mechanical — Section III-C of the Quarterly Report on this project treats the system design in considerable detail. The final set of specifications given in that report are presented in the first column of Table IV. A system based on these specifications, but with a smaller diffusion area, was built (Fig. 19) and tested. As the test proceeded, the following modifications were incorporated to produce the final system.

- As discussed in Section III-B-3-a, the tube material was changed from TFE to FEP teflon. To take advantage of the short delivery time of in-stock material, the material diameter of the insulating tube was increased from 0.078 to 0.096 cm.
- Sufficient mercury flow could be obtained only through the standard liquid mercury cathode porous tungsten impedances at pressures ranging from 40 to 60 psia, rather than the design goal of ~ 30 psia. Even with the thermally controlled needle valve ultimately used for the test, a minimum pressure of 35 psia was required for steady flow.
- At best, the mercury flow rate was erratic, the system was erratic, and the system was required to produce a bubble after one-half to two-thirds the nominal 20 min period. It was also observed that while the bubble traversed

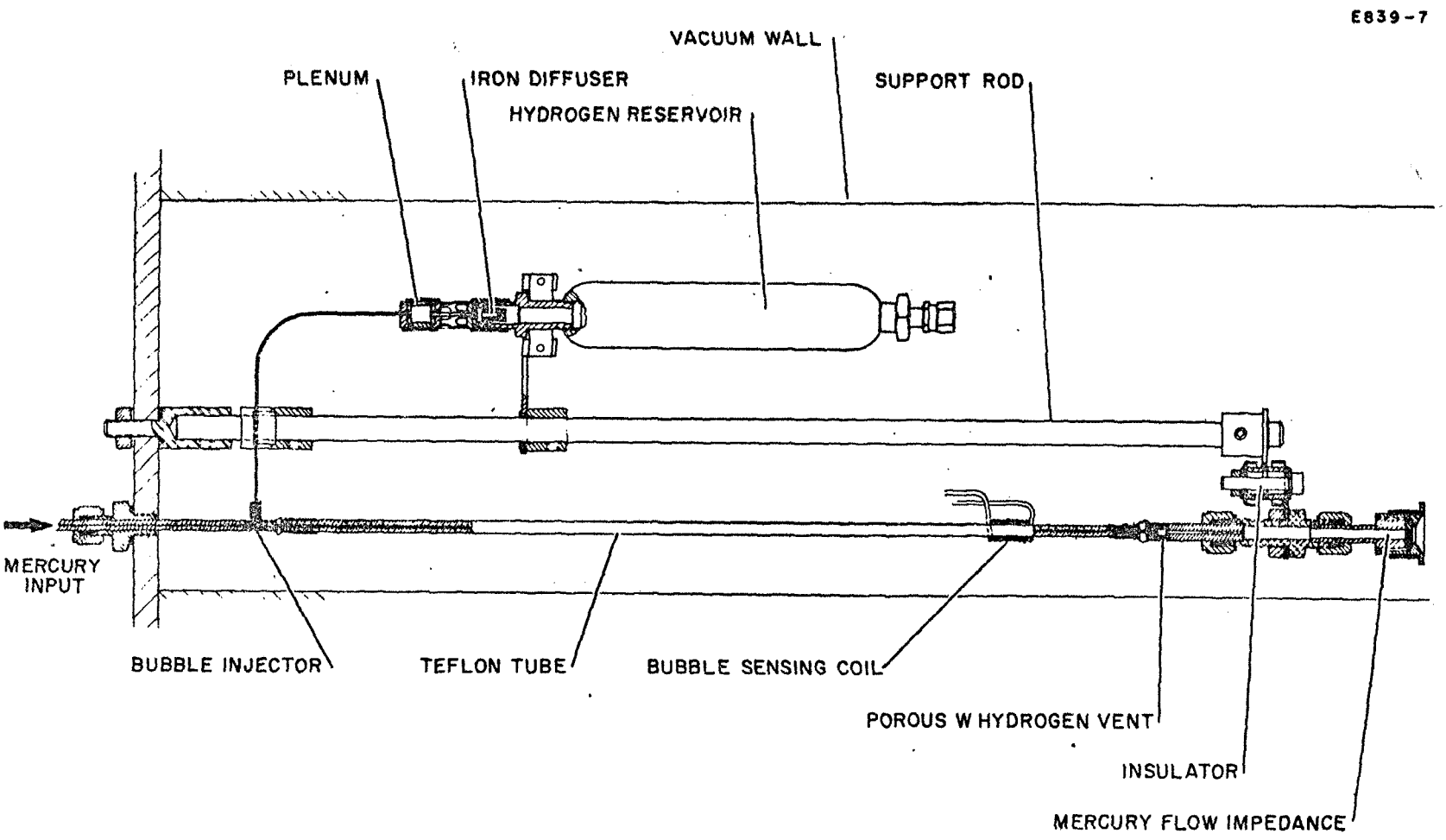

Fig. 19. Isolator system test.

TABLE IV

Isolator Parameters

Design Value	Original Design	Final Design	
		Calculated	Measured
Mercury Flow Rate, cm^3/hour	0.6	0.6	0.6
Mercury Pressure, psia	30	35	35
Insulating Tubing			
• Bore, cm	0.078	0.096	0.096
• Length, cm	30	36	36
Bubble Length, cm	0.3	1.0	1.0
Hydrogen Flow Rate, cm^3/ hour at STP	0.015	0.045	0.047
Diffuser			
• Area, cm^2	0.5	0.15	0.15
• Thickness, cm	0.2	0.15	0.15
• Temperature, ^oC	200	400 ± 30	460
Plenum			
• Volume, cm^3	0.22	0.35	0.35
• ΔT for bubble, ^oC	25	45	57
10,000 Hour Hydrogen Storage Reservoir			
• Volume, cm^3	37	90	60
• Pressure, psia	300	300	300
System Power			
• Peak, W	—	—	53
• Average, W	~3	~5	5.0

the insulating section of line it lost approximately 0.1 cm of length, presumably as a result of diffusion into the teflon tube and/or the adjacent mercury. In order to conduct a continuous test, the iron plug temperature was increased so that an average bubble length of 1.0 cm could be maintained, thus assuring the minimum length of 0.3 cm required to stand off the 5 kV. Note that the problem of irregular flow will not exist in the final system because the control circuit continually adjusts the feedline pressure to stabilize the mercury flow to the cathode at the desired rate.

The original system was modified to incorporate the above changes, and the estimated performance of this final design is given in Table IV. The principal effect of the modifications is that a higher hydrogen flow rate is required because of the increased size of the bubble. This increases the ambient temperature of the diffuser and the volume of the hydrogen reservoir. This change was largely caused by the erratic mercury flow, as explained above; this condition will not exist in closed loop operation, in which the mercury flow to the cathode is stabilized. Thus, the calculated reservoir volume of 90 cm^3 is artificially high, and a value of 40 to 50 cm^3 is more realistic for a final system. As a result of the thermal coupling between the diffuser and the plenum, the ambient plenum temperature increased with that of the diffuser, thus increasing the magnitude of the thermal transient required to generate a bubble of prescirbed length. This occurs because the thermal transient is a given fraction of the absolute ambient temperature of the plenum and because the increased

temperature difference between the plenum and feedline temperatures causes the volume of the bubble to contract more in size as it cools to feedline temperature. The increased length of the bubble of course directly increased the required temperature transient.

(2) Electrical Design — The electrical circuit was required to perform three basic functions:

- Control the diffuser temperature
- Sense the bubble position
- Thermally pulse the plenum when commanded by the bubble sensor.

The circuit and the function of each block are shown in Fig. 20. The temperature is sensed by a thermistor which is mechanically mounted in good thermal contact with the diffuser. This thermistor is used as one side of a voltage divider which determines the bias voltage on a unijunction through a diode, as shown in the figure.

When the thermistor is cold (~30°C), the unijunction acts as a switch and repetitively discharges the capacitor in its base circuit. As the thermistor is heated, its resistance decreases and the base voltage on the unijunction is reduced until the voltage across the base capacitor is no longer adequate to trigger the unijunction. The output pulses from the unijunction are used to trigger the one-shot multivibrator, which in turn operates a switching transistor which controls the power to the heater.

In summary, when the thermistor temperature is below a critical value, a series of power pulses is supplied to the heater. Above the critical temperature, no power is supplied. The circuit proved both reliable and sensitive to changes of less than 1°C at the thermistor.

The bubble sensing and trigger circuit operates as follows. The coil on the bubble sensor forms part of the tank circuit of a 27 MHz crystal controlled oscillator. As the tank circuit is determined because of the mercury in the coil being replaced by hydrogen gas, the output voltage from the oscillator decreases. This voltage is rectified, and

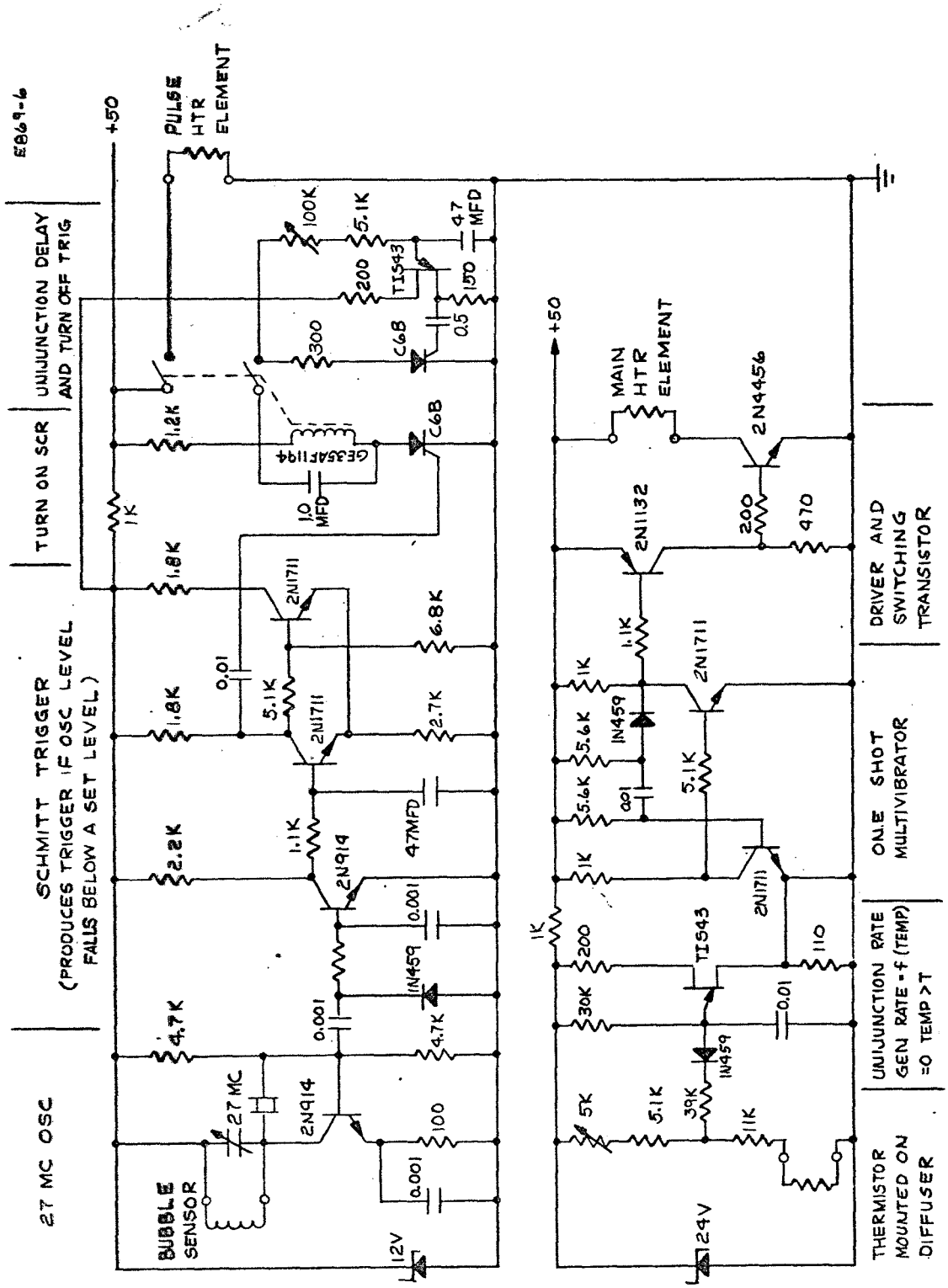

Fig. 20. Power supply and control circuit.

the resultant dc voltage is used to trigger a Schmitt trigger circuit when the voltage falls below a given level. The resulting pulse activates a SCR, which in turn closes the relay which conducts power to the plenum heater. A unijunction delay circuit which is adjustable over 0 to 10 sec is used to turn off the SCR and open the relay to terminate the pulse.

We believe the circuit approaches a minimum parts count to perform the various functions required. It can be packaged in ~4 in.^{3}.

c. Construction and Test

A layout of the test unit is shown in Fig. 19, and a photograph of the final hardware in Fig. 21. The unit was installed in a 6 in. diameter pyrex vacuum station pumped by a mechanical pump. It was found that a liquid nitrogen cold trap was required to maintain the partial pressure of mercury low enough to permit 5 kV to be applied across the isolator.

A standard LM cathode porous tungsten impedance was installed downstream of the isolator to provide the necessary flow impedance, and a pneumatically controlled mercury reservoir was used upstream to provide mercury under a controlled pressure. Later in the program a temperature controlled needle valve was substituted for the impedance to provide a continuous control over the flow impedance. Neither of these devices was entirely satisfactory, and the seemingly trivial task of maintaining constant mercury flow rate for the desired test period proved to be the most difficult feature of the test.

Two tests of greater than 100 hour duration were run. The first was a 120 hour continuous test which was run before the liquid nitrogen cold trap was installed on the system. Shortly after the test began, it was found that voltages greater than 4 kV caused a glow discharge between the high voltage end of the isolator and the collector. Because of this, the test was run at 4 kV and was voluntarily terminated after 120 hours. Because of the design specification for operation at 5 kV, the vacuum station was modified to accommodate a cold trap so that the mercury vapor pressure could be maintained low enough to permit the system to sustain 5 kV.

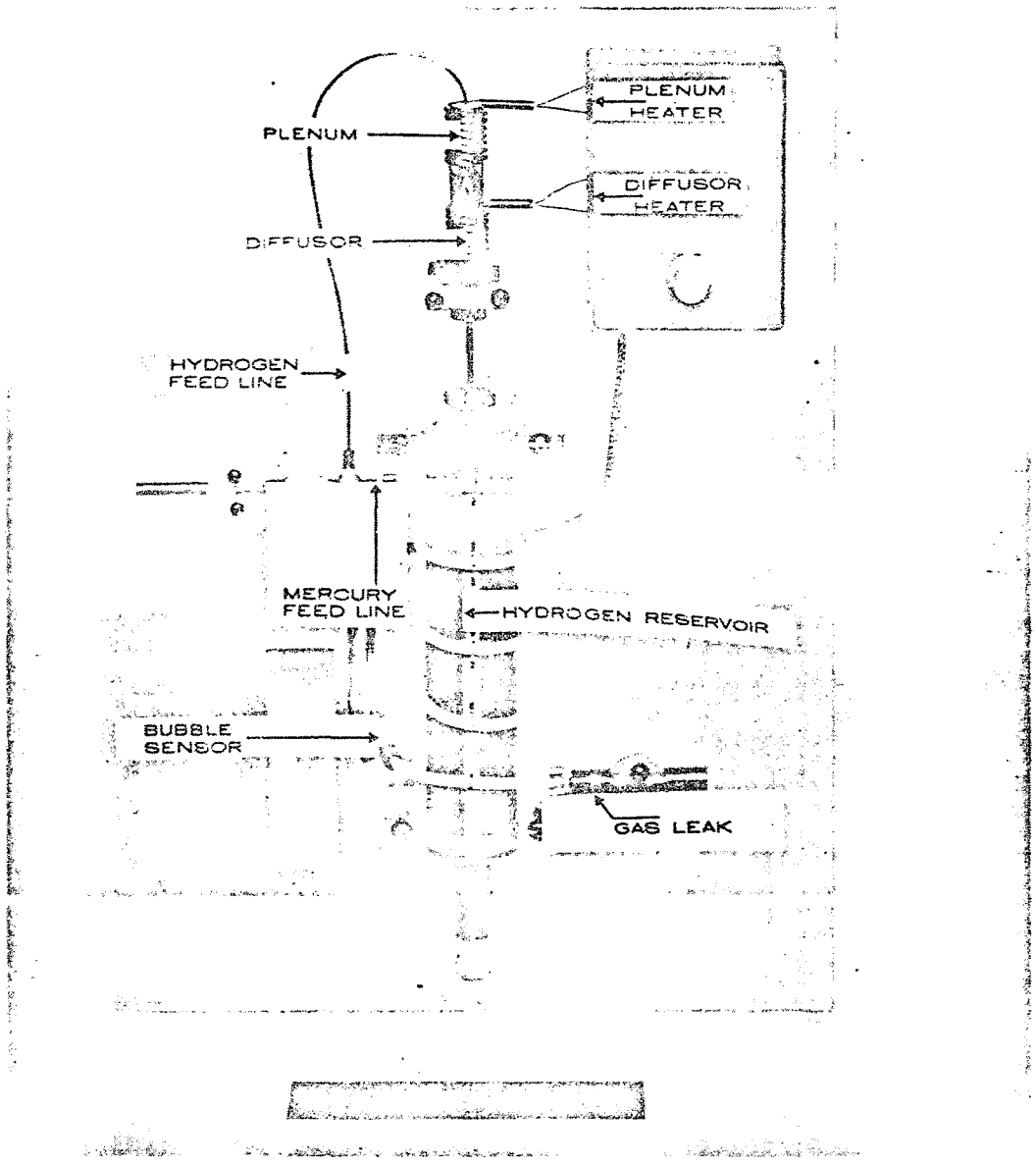

Fig. 21. Bubble isolator system.

With this system, 243 hours at 5 kV were accumulated without electrical breakdown during normal operation. The typical operating parameters are presented in Table IV. Because of the problem of adjusting and stabilizing the mercury flow, the flowrate could not be maintained constant during this period; on several occasions it stopped entirely for periods of from 1 to 15 hours. The bubble which was in the tube when flow stopped would slowly shrink because of the diffusion of hydrogen into the mercury; after approximately 4 hours, a short circuit developed.

The system was restarted by reinitiating the mercury flow and providing a single manual trigger pulse to generate the first bubble. At all times when a gas bubble was in the line, the leakage current was less than 0.1 mA.

These tests demonstrated satisfactory performance of all isolator components and of the entire system.

5. Design Improvements for Future Systems

The following improvements are suggested for future systems:

- Design for a larger diffuser area, thus permitting lower temperature operation
- Design diffuser cavity and plenum as a single unit, with one heater which could provide both the necessary ambient temperature for the diffuser and the thermal pulse to create the bubble
- Design for a longer thermal pulse at lower power, thus reducing the peak power requirement of the system.

6. Flight Hardware Specifications

Based on the program described above, the design of flight hardware is considered feasible. The estimated physical characteristics of such a device are as follows

- Weight 0.8 lb
- Power
  - Peak 10 W
  - Average 3 W

C. ELECTROMAGNETIC PRESSURIZER

As explained above, it is necessary to be able to adjust the mercury pressure in the propellant line leading to each LM cathode so that the flow to the individual cathodes can be regulated. In a system where individual cathodes are fed through isolators from a common propellant manifold, a pressure regulating device is required in series with each isolator. The only practical method of accomplishing this is through the use of electromagnetic forces. It was required under the contract that such devices be investigated in sufficient detail that reasonable estimates of the weight and efficiency could be made.

It is required that the pressurizer work in a low flow high pressure application and accept power at the highest possible voltage. The latter is important from a power conditioning standpoint because high current, low voltage dc supplies are both inefficient and difficult to regulate.

Figure 22 is a conceptual drawing of an electromagnetic pump and Fig. 23 is an artist's sketch of the design fabricated to meet the design requirements. Figures 24 and 25 show the actual components of a unit which produces pressure heads of ± 1 atm at 12 A. Note particularly that the electrical contacts are designed to have a large surface area and are platinum plated so that they are wet by the mercury; both features are designed to reduce the potential between the mercury and the electrode. The magnetic circuit is efficient because leakage flux is

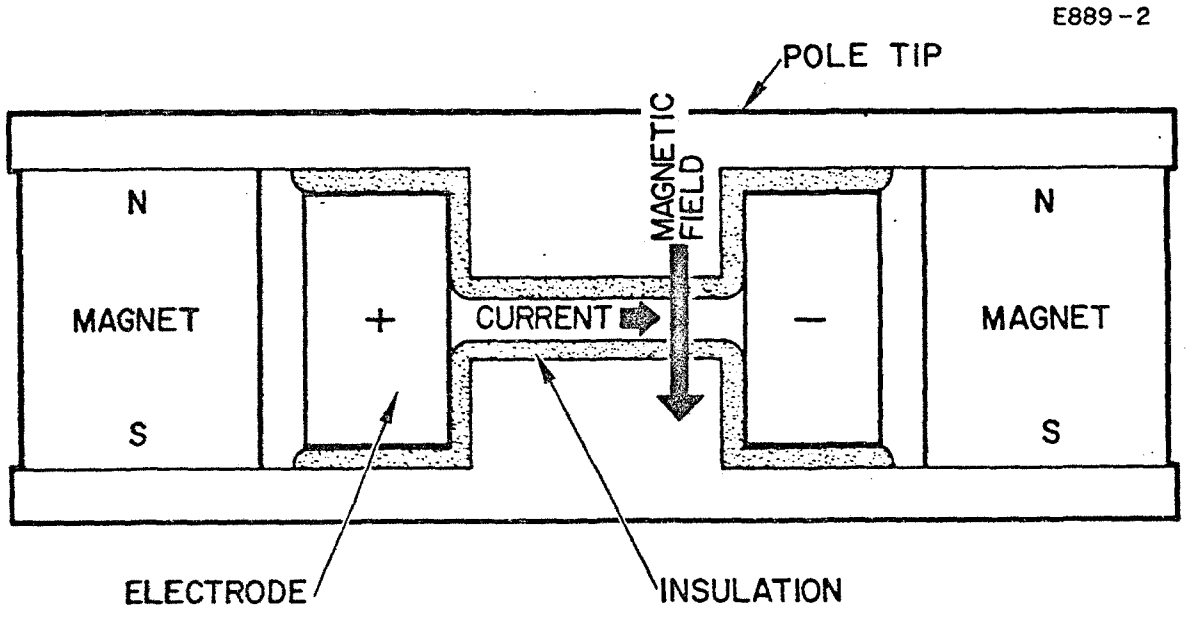

Fig. 22. Basic electromagnetic pump concept.

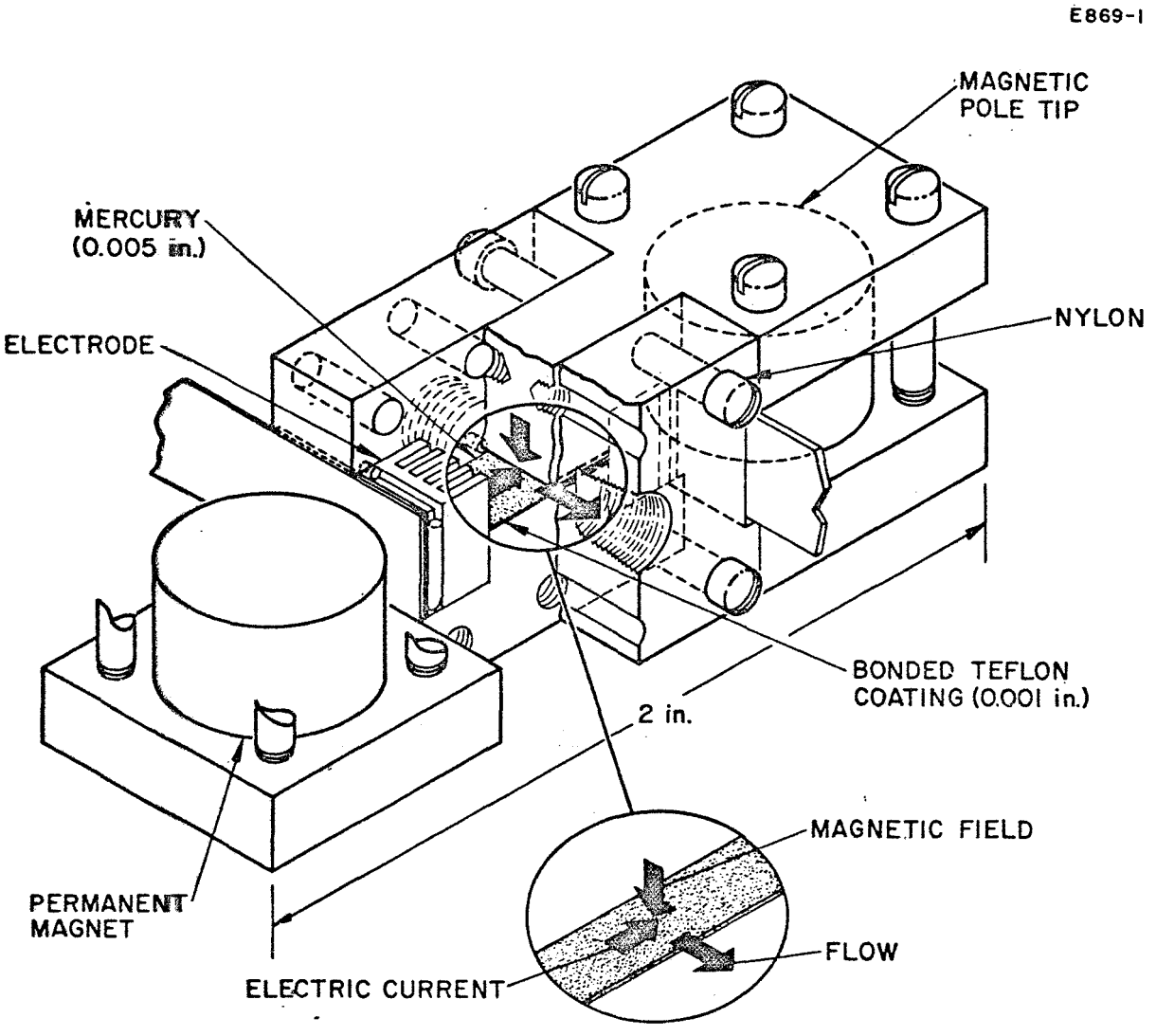

Fig. 23. Sectional view of electromagnetic pump.

M 5593

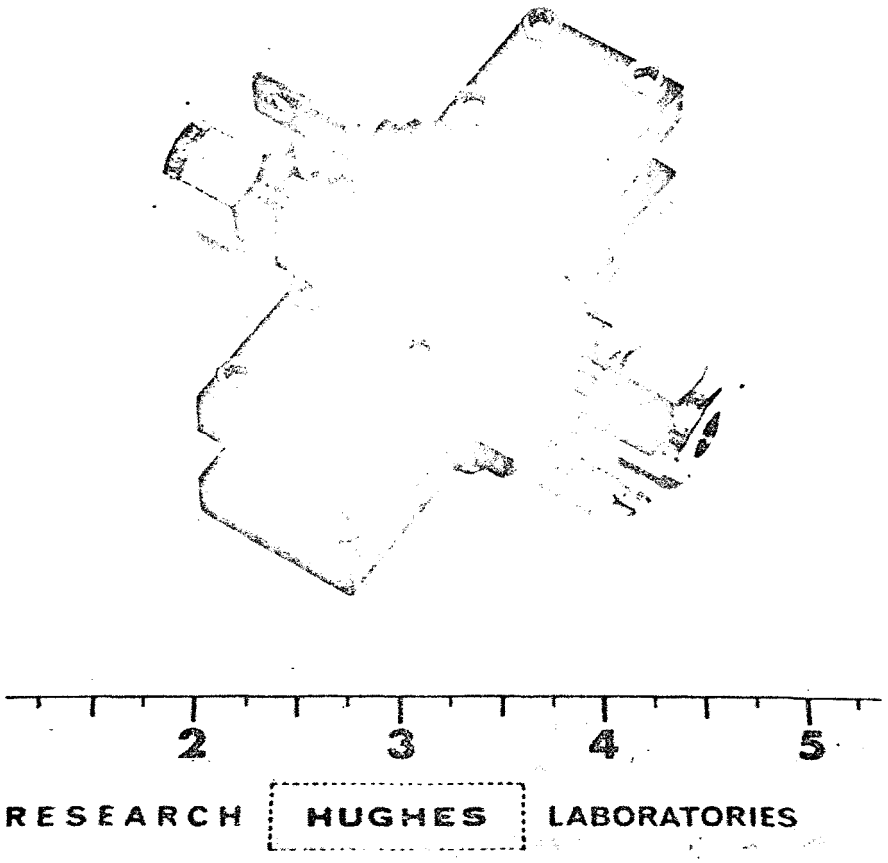

Fig. 24. Photo of electromagnetic pump.

M 5595

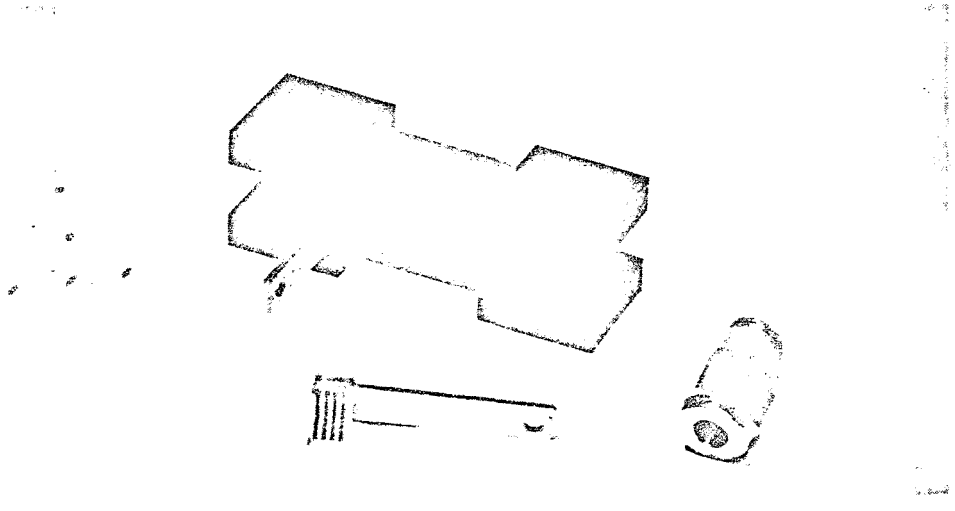

Fig. 25. Electromagnetic pump components.

relatively small and the poles may be precisely spaced. The pole tips themselves are coated with a thin layer of teflon bonded to the surface. They thus serve as an insulating channel through which the mercury and (in a perpendicular direction) the electric current flow; the I^2R heat generated in the mercury is still allowed to be readily dissipated, although the mercury flow may approach zero.

Two pumps which differed only in seal design were fabricated and tested. The head produced was typically over 80% of the theoretical maximum calculated from a knowledge of the pump dimensions, magnetic field, and the measured current flow. Details of the static head and flow are shown in Fig 26.

Based on these tests, it was concluded that an electromagnetic pump capable of producing a static pressure head of ±1 atm can be reliably designed and constructed in the current state of the art. The particular unit, which was designed for flexibility and ease of assembly rather than minimum weight, weighed 250 g. Based on this design, the estimated performance of a model designed for flight application is

• Size	2 cm x 2 cm x 5 cm
• Weight	100 g (0.22 lb)
• Maximum ΔP	±2
• Electrical Characteristics at 15 psi	
I, A	10
V, V	0.2
P, W	2

4. Insulating Valve

Systems incorporating an insulating valve are discussed above. As with the pressurizer, the contractual requirement was to estimate the weight and reliability of such a device. A number of concepts were investigated and experimental hardware were fabricated so that a typical design could be tested in which the closing motion of the valve

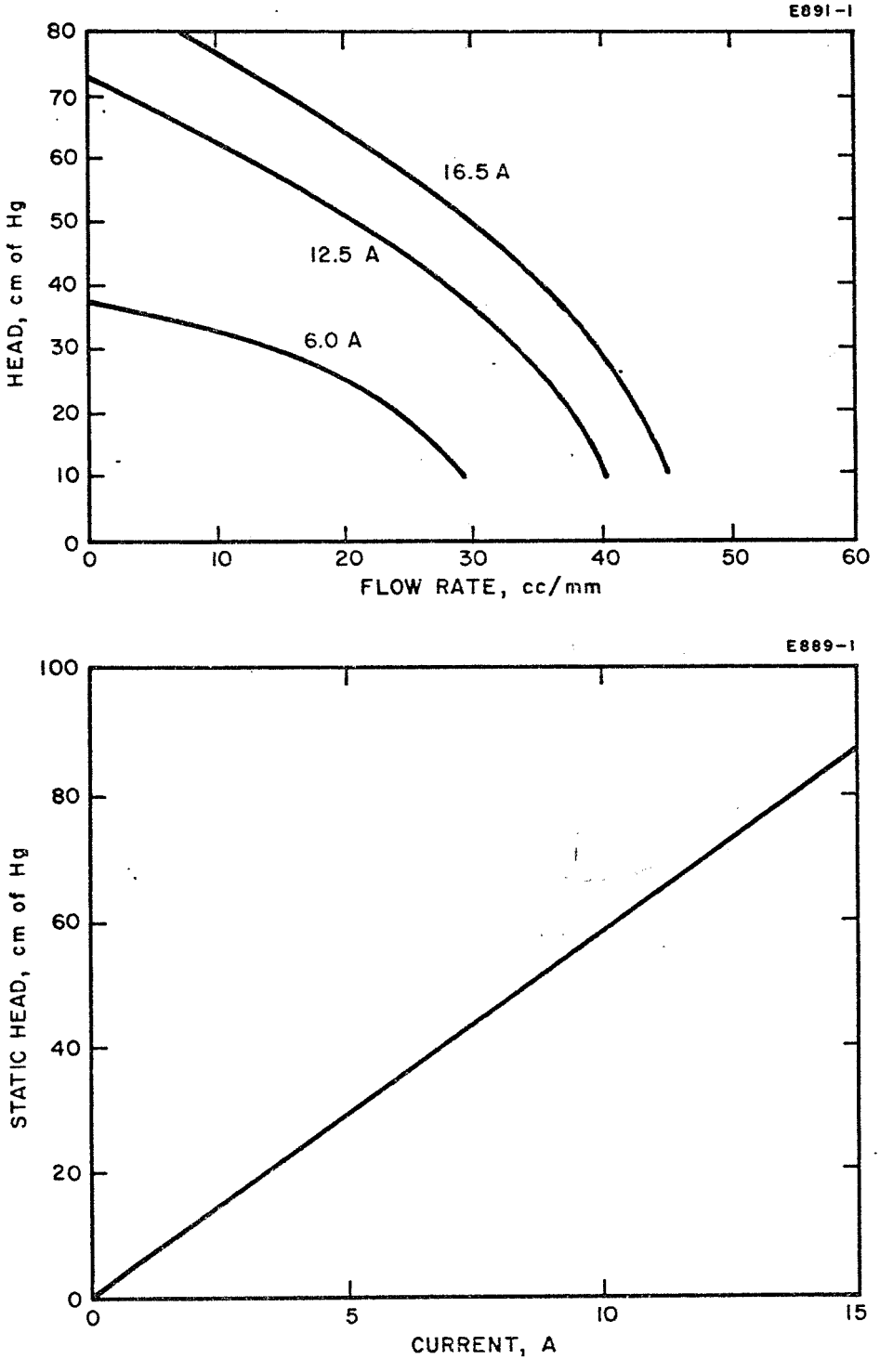

Fig. 26. Electromagnetic pump performance curves.

wiped or scraped the valve seat free of mercury as it closed. When the valve was closed the clean valve seat both stopped the mercury flow and provided the insulation in the mercury line necessary to withstand the beam voltage (~5 kV). For the reasons discussed above for solid isolators, all such valves failed. If the fit between mating parts was sufficiently good that no mercury remained between mating surfaces, very large mechanical forces were required to close the valve. If the fit was loose, a thin film of mercury remained between mating surfaces and insulation was not achieved. Once one arc-over occurred, the surface insulating properties were destroyed, and the valve would no longer function.

The above failure led to a design in which the insulating and valving actions were performed by separate components — a standard valve, and the insulating device described below. Figure 27 shows the basic concept, which is an insulating sphere in an elastomeric section of the mercury line. At zero pressure (when the mechanical valve is shut) the elastomeric tube contracts around the ball and forces the mercury out of the intervening region, thus interrupting the electrical continuity. Under high pressure the tube expands, and mercury can flow past the ball.

A functional design based on this principle (Fig. 28) was fabricated and tested. The elastomer was a length of 1/4 in. i.d., rubber tubing and all other parts machined from Kel-F. Only one unit was fabricated. It was found that flow started and stopped reproducibly at 17 psi mercury pressure, with little hysteresis. For the first electrical test the flow was stopped with an upstream valve and the system was allowed to sit for 1 hour. High voltage was applied through a limiting resistor, with breakdown occurring at ~4700 V. The voltage was removed and the flow restarted and then stopped. Voltage was immediately reapplied, and breakdown occurred at ~2000 V. It was not clear from the experiment whether this lower breakdown threshold was a result of the shorter "rest period" during which the mercury was extruded from the insulating region, or a result of surface tracking caused by the earlier breakdown.

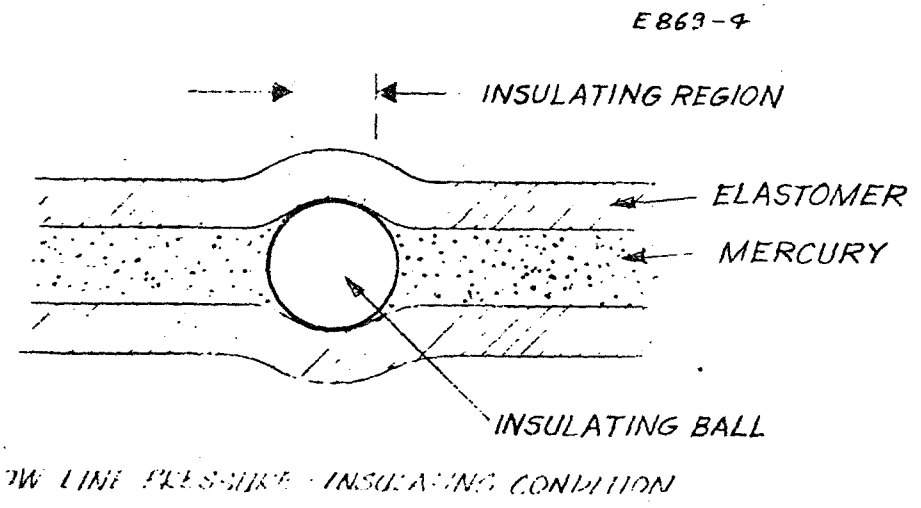

(a)

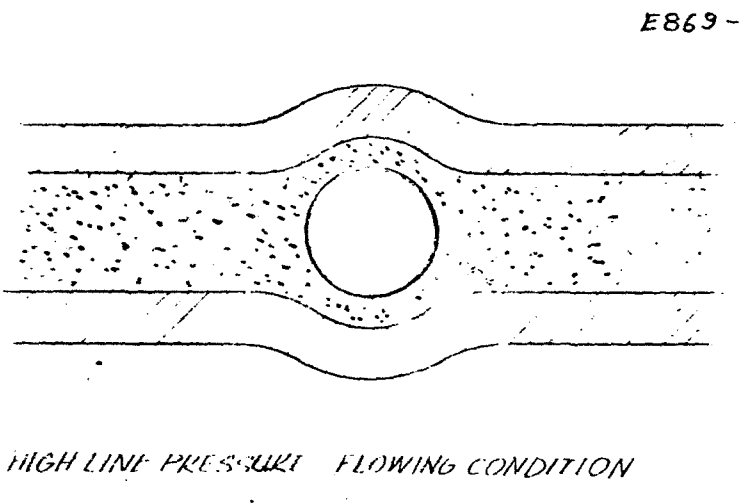

(b)

Fig. 27. Insulating device. (a) Insulating configuration; the mercury is squeezed from the region between the ball and the tube, providing an electrically insulating region. (b) Open configuration; at high mercury pressures the tube expands and mercury flows past the ball.

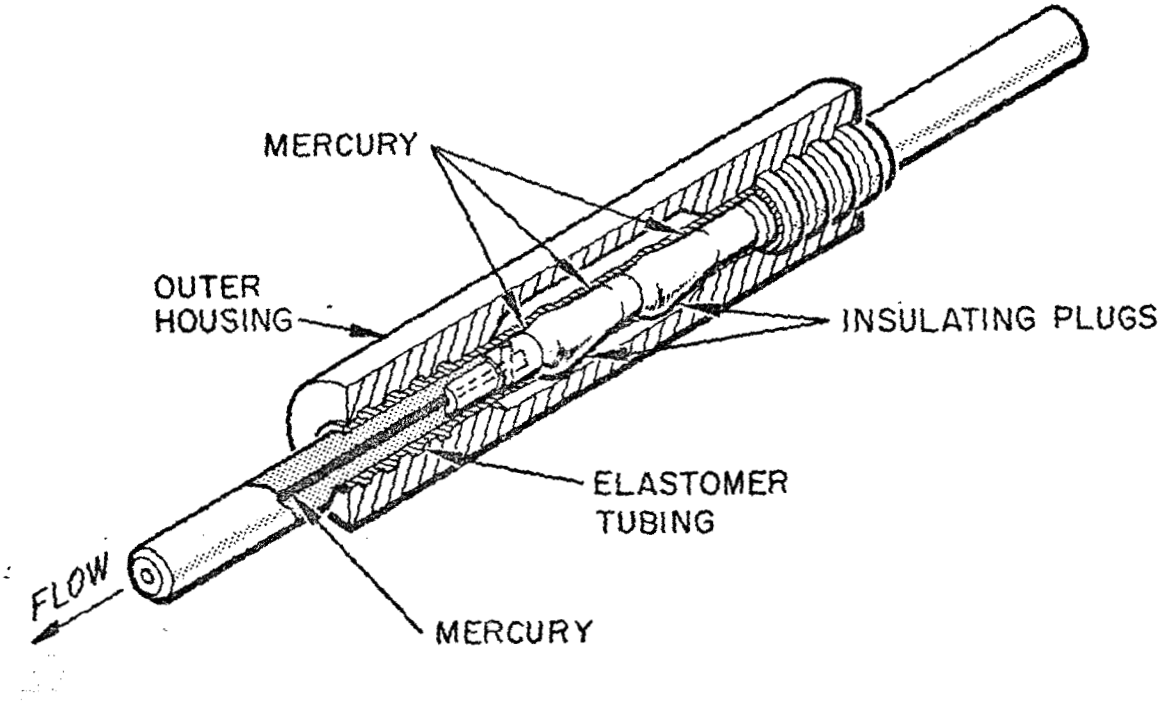

Fig. 28. Insulating valve.

If this concept is to be developed into a functional unit, much more intensive effort should be devoted to it. The basic idea appears sound, however, and weight estimates based on this concept may be made reliably.

SECTION IV

SUMMARY AND CONCLUSIONS

Eight modularized ion propulsion systems based on the liquid mercury cathode, electron-bombardment thruster were evaluated to determine the effect of various degrees of electrical isolation on system reliability, weight, and operational characteristics. Seven of these systems employed some degree of isolation, provided either by an isolator component or an insulating valve in the feed line of each thruster. An additional variation in these system designs was the use of an electromagnetic pump or the positive expulsion system of a reservoir to provide flow control to the individual thrusters. The remaining system employed no isolation and was used as a reference design.

In order that a proper evaluation of these systems could be made, operational models of three unique components — a liquid mercury isolator, an insulating valve, and an electromagnetic pressurizer — were designed and tested. These designs, together with past experience in the design and test of thrusters, propellant reservoirs, distribution systems, and power conditioning and control systems, provided the basis of the quantitative estimates of reliabilities and weights of the various systems considered.

The results of the study showed that for a constant-weight criterion, the reliabilities of the systems which provide some degree of isolation were greater (e.g., 0.88 versus 0.83) than that of the non-decoupled reference system. The major difference was the existence in the reference system of failure modes in the individual thruster and power conditioning subsystems which proved catastrophic to the whole system. The reliabilities of the seven systems which provided some degree of isolation were, to first order, equal. Therefore, the choice of design from among these seven could be based on other considerations,

such as degree of isolation provided, simplicity of operational characteristics (e.g., propellant transfer requirements, procedure in event of thruster or power conditioner trip, etc.), and availability of components. On this basis, the system which employed an isolator component and EM pump in each thruster feed line was found to be superior to the others. For example, this configuration provides total electrical isolation among all subsystems, requires no complex operational procedure in the event of a subsystem failure, and uses components which have been developed or are under development.

A final important conclusion is that a modularized propulsion system can be quite reliable. For example, based on estimated failure rates, the system reliability for the 1973 Jupiter flyby reference mission was 0.88. This relatively high reliability is obtained at acceptable weight penalties because of the partial redundancy which modularization allows. However, it should be noted that when propellant is included in redundant tanks (a probable necessity), the reservoir redundancy becomes the major source of weight penalty. In order to reduce this potentially serious problem, reservoir reliabilities should be raised to high levels, even though the individual tank weight might experience a relatively large percentage increase.

REFERENCES

1. "Solar Powered Electric Propulsion," Program Summary Report, JPL Contract No. 951144, Hughes Aircraft Company, December 1966.

2. "Reliability Analyses of Modularized Power Conditioning and Control Systems for Ion Engines," Final Report, JPL Contract No. 951144, Hughes Aircraft Company, November 1966.

3. H.J. King, et al., "Electron Bombardment Thrusters Using Liquid Mercury Cathodes," AIAA Preprint 66-232, 1966.

4. P. Reader, NASA JPL, private communication.

5. F. Ehrenkranz, Phys. Rev. 55, 219 (1939).

6. E. Lowery, Ann. N.Y. Acad. Sci. 65, 357 (1957).

7. C. Conger, NASA-LeRc, private communication to R.C. Knechtli.

8. S. Dushman, Scientific Foundation Transactions on Vacuum Technology, 2nd ed. (Wiley and Sons, New York, 1965) p. 573.

9. C. Smithells and C. Ransley, Proc. Roy. Soc. (London) A150, 172 (1935).

APPENDIX

COMPONENT WEIGHTS AND FAILURE RATES

The failure rates presented in this appendix are based on data obtained from Technical Report RADC-TR-66-828, "RADC Unanalyzed Nonelectronic Part Failure Rate Data, Interim Report NEDCO." This report is an extensive compilation of failure rates for various components in airborne, ship, and ground applications. It also contains a limited amount of space and missile application data.

Since no reliability data exist for many of the components used in an ion propulsion system, the component failure rates of similar equipment used in "airborne" applications have been selected for this study. Because components are subjected to far greater stress in an airborne environment than in the space environment (other than the relatively short boost phase), the failure rates selected were adjusted by a "K" factor of 1/200. This factor, which is suggested in Martin Company's "Reliability Data Handbook" to convert data from airborne to space environment, brings the NEDCO I failure rates into good agreement with the "generic" failure rate range of the Martin data. Furthermore, experience by the HAC Space Systems Division has shown that observed failure rates are in good agreement with the Martin data, scattered randomly between the specified upper and lower limits. In final analysis, the NEDCO I data were used because they are more extensive than any other compilation of mechanical reliability data available at present.

The component weight breakdown presented in this appendix was based on specific ion propulsion system components designed and/or developed at Hughes Research Laboratories.

Following are the detailed weight and failure rate estimates for all components used in the system designs considered in this program.

THRUSTER

Component	Unit Failure Rate, $\lambda/10^6$ Hour	Number Used	Total Failure Rate, $\lambda/10^6$ Hour	Unit Weight, lb	Total Weight, lb
1. Accel Electrode (Mo)*	0.300	1	0.300	1.15	1.15
2. Screen Electrode (Mo)*	0.350	1	0.350	0.95	0.95
3. Insulator - Ceramic*	0.020	12	0.024	<0.01	0.08
4. Shield-Insulator, Inner*	0.003	12	0.036	>0.01	0.14
5. Shield-Insulator, Outer*	0.003	12	0.036	<0.02	0.21
6. Neutralizer-Hollow Cathode	—	—	—	—	—
a. Heater	0.220	1	0.220	<0.01	0.01
b. Starting Anode	0.350	1	0.350	0.02	0.02
c. Shell	0.100	1	0.100	0.02	0.02
d. Liner, Oxide	0.150	1	0.150	0.01	0.01
e. Terminals, Heater	0.010	2	0.020	0.01	0.02
f. Tubing-Hg Vapor	0.030	1	0.030	0.03	0.03
g. Bellows	0.080	1	0.080	<0.01	0.01
h. Insulator-Mounting	0.020	6	0.120	>0.01	0.07
i. Screen-Mounting	0.025	2	0.050	<0.01	0.01
j. Joints Welded	0.005/in.	2 in.	0.010	—	—
k. Joints Brazed	0.005/in.	1 in.	0.010	—	—
l. Shields-Insulator, Inner	0.003	6	0.018	<0.01	0.04
m. Shields-Insulator, Outer	0.003	6	0.018	0.01	0.06
n. Nuts-Acorn	0.020	4	0.080	<0.01	0.02
7. Studs-Electrode Mtg. No. 10	0.025	6	0.150	>0.01	0.07
8. Nuts-Acorn	0.005	12	0.060	<0.01	0.05
9. Bracket-Electrode Mtg.	0.050	6	0.300	0.03	0.18
10. Screen No. 10	0.025	12	0.300	<0.01	0.06
11. Magnets-Permanent Bar	0.030	12	0.360	0.20	2.40
12. Ring-Outer Shell Forming	0.025	2	0.050	0.74	1.48
13. Shell	0.100	1	0.100	0.77	0.77
14. Main Support Strut-Outer Shell	0.050	3	0.150	0.15	0.45
15. Bracket Support	0.010	3	0.030	0.02	0.06
16. Insulator-Anode Shell	0.020	6	0.120	<0.01	0.03
17. Stud-Anode-Shell Support	0.030	6	0.180	<0.01	0.04
18. Weld Joints - Sealing	0.005/in.	165	0.825	—	—
19. Weld Joints - Structural	0.002/in.	95	0.190	—	—
20. Ring-Anode Forming	0.025	2	0.050	0.15	0.30
21. Shell-Anode	0.150	1	0.150	0.75	0.75
22. Ring-Manifold	0.100	1	0.100	0.25	0.25
23. Seal-Labyrinth	0.040	1	0.040	0.03	0.03
24. Insulator Assembly*	0.050	1	0.050	0.09	0.09
25. Seal-Hg Inlet	0.100	1	0.100	0.16	0.16
26. Screws	0.025	4	0.100	<0.01	0.03
27. Weld Joints-Sealing	0.005/in.	13 in.	0.065	—	—
28. Cathode	1.593	1	1.593	0.52	0.52
29. Plate, Back	0.100	1	0.100	0.29	0.29
30. Weld Joint, Sealing	0.005/in.	35 in.	0.175	—	—
Total			7.340		10.86

*Items which can cause catastrophic system failure.

MANIFOLD-WELDED – ~6 FT LONG - 8 OUTLETS

Component	Unit Failure Rate, $\lambda/10^6$ Hour	Number Used	Total Failure Rate, $\lambda/10^6$ Hour	Unit Weight, lb	Total Weight, lb
1. Tubing	0.090	1	0.090	0.60	0.60
2. Weld Joints	0.005/in.	5 in.	0.025	—	—
3. Boss, Welded	0.050	8	0.400	0.03	0.24
Total			0.515		0.84

SOLENOID VALVE – CONVENTIONAL

Component	Unit Failure Rate, $\lambda/10^6$ Hour	Number Used	Total Failure Rate, $\lambda/10^6$ Hour	Unit Weight, lb	Total Weight, lb
1. Solenoid Coil	0.250	1	0.250		0.11
2. Spring	0.550	1	0.550		<0.01
3. Screw, Adjustment	0.450	1	0.450		<0.01
4. Static Seal	0.155	2	0.310		<0.01
5. Dynamic Seal	0.890	1	0.890		0.03
6. Connector, Electrical	0.050	1	0.050		0.03
Total			2.500		0.18

INSULATING VALVE

Component	Unit Failure Rate, $\lambda/10^6$ Hour	Number Used	Total Failure Rate, $\lambda/10^6$ Hour	Unit Weight, lb	Total Weight, lb
1. Ball Structure, Plastic	0.050	1	0.050	—	<0.01
2. Tube, Plastic, Inlet and Outlet	0.150	2	0.300	—	<0.01
3. Tubing, Latex, Unreinforced	0.500	1	0.500	—	<0.01
4. Housing, Structure, Plastic	0.150	1	0.150	0.02	0.02
5. Clamps	0.100	2	0.200	0.02	0.04
Total			1.200		0.07

ISOLATOR SYSTEM – H_2 BUBBLE INJECTION

Component	Unit Failure Rate, $\lambda/10^6$ Hour	Number Used	Total Failure Rate, $\lambda/10^6$ Hour	Unit Weight, lb	Total Weight, lb
1. Tank-High Pressure Gas	0.065	1	0.065	0.12	0.12
2. Valve-Filler	0.500	1	0.500	0.06	0.06
3. Plug-Welded-Diffusion	0.005	1	0.005	0.03	0.03
4. Heater and Control	0.220	2	0.440	0.18	0.36
5. Tubing, Metal	0.090	3	0.270	0.02	0.06
6. Welded Joints	0.005/in.	4	0.020	—	—
7. Tubing, Reinforced Plastic	0.050	1	0.050	0.06	0.06
8. Clamps-Tubing	0.010	2	0.020	0.01	0.02
9. Bleed-Gas	0.100	1	0.100	0.03	0.03
10. Fittings	0.725	2	1.450	0.04	0.08
Total			2.920		0.82

EM PUMP

Component	Unit Failure Rate, $\lambda/10^6$ Hour	Number Used	Total Failure Rate, $\lambda/10^6$ Hour	Unit Weight, lb	Total Weight, lb
1. Magnets	0.030	2	0.060	0.05	0.10
2. Pole Shoes	0.100	2	0.200	0.15	0.30
3. End Plates-Plastic	0.020	2	0.040	0.03	0.06
4. Electrodes	0.500	2	1.000	0.02	0.04
5. Seal, Static-Press	1.000	2	2.000	<0.01	<0.01
6. Coating, Insulating-Elect.	0.425	2	0.850	—	—
7. Screws	0.025	14	0.350	<0.01	0.05
8. Fittings	0.725	2	1.450	0.04	0.08
Total			5.950		0.64

RESERVOIR – GAS PRESSURIZED, BLADDER TYPE TITANIUM -0.010 MIN. WALL

Component	Unit Failure Rate, $\lambda/10^6$ Hour	Number Used	Total Failure Rate, $\lambda/10^6$ Hour	Unit Weight, lb	Total Weight, lb
1. Gasket	0.035	1	0.035	0.02	0.02
2. Fittings	0.725	4	2.900	0.04	0.16
3. Bladder	0.130	1	0.130	0.22 - 0.39	0.22 - 0.39
4. Flanges	0.205	2	0.410	Noted 10	—
5. Tubing, Metal	0.090	2	0.180	0.01	0.02
6. Heater and Control	0.220	1	0.220	0.25	0.25
7. Valve, Filler	0.500	1	0.500	0.06	0.06
8. Valve, Solenoid	2.500	1	2.500	0.25	0.25
9. Tank, High Press Gas	0.065	1	0.065		
a. 86.5 lb Hg Reservoir				0.16	0.16
b. 173 lb Hg Reservoir				0.31	0.31
c. 270 lb Hg Reservoir				0.48	0.48
d. 433 lb Hg Reservoir				0.76	0.76
e. 865 lb Hg Reservoir				1.50	1.50
10. Ends, Hemispherical and Flange	0.050	2	0.100		
a. 86.5 lb Hg Reservoir				0.29	0.58
b. 173 lb Hg Reservoir				0.44	0.88
c. 270 lb Hg Reservoir				0.63	1.26
d. 433 lb Hg Reservoir				0.88	1.76
e. 865 lb Hg Reservoir				1.81	3.62
11. Cylindrical Section	0.100	2	0.200		
a. 86.5 lb Hg Reservoir				0.11	0.22
b. 173 lb Hg Reservoir				0.12	0.24
c. 270 lb Hg Reservoir				0.13	0.26
d. 433 lb Hg Reservoir				0.15	0.30
e. 865 lb Hg Reservoir				0.22	0.44
12. Welded Joints	0.005/in.				
a. 86.5 lb Hg Reservoir		73 in.	0.365		
b. 173 lb Hg Reservoir		91 in.	0.455		
c. 270 lb Hg Reservoir		105 in.	0.525		
d. 433 lb Hg Reservoir		116 in.	0.580		
e. 865 lb Hg Reservoir		151 in.	0.755		
13. Screws	0.025				
a. 86.5 lb Hg Reservoir		20	0.500	0.01	0.20
b. 173 lb Hg Reservoir		24	0.600	0.01	0.24
c. 270 lb Hg Reservoir		28	0.700	0.01	0.28
d. 433 lb Hg Reservoir		32	0.800	0.01	0.32
e. 865 lb Hg Reservoir		36	0.900	0.01	0.36
Totals - Hg Reservoir Syst.					
a. 86.5 lb Capacity			8.105		2.36
b. 173 lb Capacity			8.295		2.87
c. 270 lb Capacity			8.465		3.50
d. 433 lb Capacity			8.620		4.45
e. 865 lb Capacity			8.895		7.35